COLITIS

Vagal stimulation ameliorates murine colitis by regulating SUMOylation

Ayman Youssef[1,2]†, Ata Ur Rehman[1], Mohamed Elebasy[1], Jatin Roper[3], Shehzad Z. Sheikh[4], Jorn Karhausen[1,5], Wei Yang[1]*, Luis Ulloa[1]*

Inflammatory bowel diseases (IBDs) are chronic debilitating conditions without cure, the etiologies of which are unknown, that shorten the lifespans of 7 million patients worldwide by nearly 10%. Here, we found that decreased autonomic parasympathetic tone resulted in increased IBD susceptibility and mortality in mouse models of disease. Conversely, vagal stimulation restored neuromodulation and ameliorated colitis by inhibiting the posttranslational modification SUMOylation through a mechanism independent of the canonical interleukin-10/α7 nicotinic cholinergic vagal pathway. Colonic biopsies from patients with IBDs and mouse models showed an increase in small ubiquitin-like modifier (SUMO)2 and SUMO3 during active disease. In global genetic knockout mouse models, the deletion of *Sumo3* protected against development of colitis and delayed onset of disease, whereas deletion of *Sumo1* halted the progression of colitis. Bone marrow transplants from *Sumo1*-knockout (KO) but not *Sumo3*-KO mice into wild-type mice conferred protection against development of colitis. Electric stimulation of the cervical vagus nerve before the induction of colitis inhibited SUMOylation and delayed the onset of colitis in *Sumo1*-KO mice and resulted in milder symptoms in *Sumo3*-KO mice. Treatment with TAK-981, a first-in-class inhibitor of the SUMO-activating enzyme, ameliorated disease in three murine models of IBD and reduced intestinal permeability and bacterial translocation in a severe model of the disease, suggesting the potential to reduce progression to sepsis. These results reveal a pathway of vagal neuromodulation that reprograms endogenous stress-adaptive responses through inhibition of SUMOylation and suggest SUMOylation as a therapeutic target for IBD.

INTRODUCTION

Inflammatory bowel diseases (IBDs) are idiopathic, chronic, debilitating conditions affecting nearly 7 million people worldwide. The two major IBDs include ulcerative colitis (UC) with continuous inflammation through the colon, and Crohn's disease (CD) with patchy inflammation in the whole digestive tract from the mouth to the anus. The Centers for Disease Control and Prevention estimates that IBD affects nearly 4 million Americans, with epidemiological studies reporting a 50% increase in IBD prevalence in the last 15 years (*1*, *2*). There is no cure for IBD, and IBDs cause inflammation, colon perforation, and increased risk of both sepsis and cancer and can shorten patients' lifespans by around 10% (*3*–*5*). Current anti-inflammatory therapies reduce the need for surgery, but patients lose responsiveness over time and experience side effects and relapses that affect their quality of life and health (*6*–*8*). Therefore, there is a need for alternative therapies to treat these diseases.

Psychological stress is a main factor in the six leading causes of death (*9*). A typical example is the implications of stress in IBDs, especially UC, which was originally regarded as a psychosomatic disorder (*10*, *11*). Stress directly affects immune homeostasis through the modulation of the nervous system. Previous studies suggested that stress may cause autonomic dysfunction affecting the parasympathetic system, and deficient vagal tone is increasingly recognized as a physiological marker for stress (*12*–*14*). We reported that vagal and noncholinergic sciatic nerve stimulations curb systemic inflammation and improve organ function in experimental sepsis (*15*–*17*). Bioelectronic medicine is an emerging field based on nerve stimulation to control organ function and restore immune homeostasis in infectious and inflammatory disorders. Several pilot studies of nerve stimulation in infectious and inflammatory disorders such as polyneuropathies (NCT04053127), heart failure (NCT03425422), rheumatoid arthritis, and traumatic brain injury (NCT02974959) are underway, and some have provided promising results (*18*, *19*). Two pilot studies have reported that vagal stimulation can improve clinical outcomes in patients with CD (*20*–*22*). One study showed that 1-year vagal stimulation treatment improved endoscopic scores in half of the 16 patients with CD who participated (*21*), and the other study reported remission in six of nine patients with CD, but the other three patients experienced worsened of their disease (ClinicalTrials.gov identifier: NCT01569503) (*20*, *22*). These results highlight the need for mechanistic studies to better understand the reasons for patient nonresponse or worsening and to improve treatment efficacy while avoiding surgical nerve manipulation.

Although the pathogenesis of IBDs is currently unknown, we and others have reported SUMOylation as an emerging stress-adaptive response to safeguard intestinal integrity, a tissue particularly challenged by its bacterial environment (*23*–*25*). SUMOylation refers to the covalent, reversible conjugation of target proteins to small ubiquitin-like modifier (SUMO) proteins as a posttranslational modifier to regulate protein interactions and functions (*26*). SUMOylation is critical for survival, and total inhibition of SUMOylation by genetic ablation of *Ubc9* (ubiquitin-conjugating enzyme 9 that functions as the sole E2-conjugating enzyme required for SUMOylation) causes early embryonic death (*27*). SUMOylation is highly responsive to endogenous and environmental stressors and coordinates critical signaling pathways and transcriptional factors to reprogram immune cells at multiple levels (*28*, *29*). A previous study reported

[1]Center for Perioperative Organ Protection, Department of Anesthesiology, Duke University Medical Center, Durham, NC 27710, USA. [2]Autonomic Dysfunction Center, Vanderbilt University Medical Center, Nashville, TN 37232, USA. [3]Department of Medicine, Division of Gastroenterology, Duke University, Durham, NC 27710, USA. [4]University of North Carolina, Center for Gastrointestinal Biology and Disease, University of North Carolina at Chapel Hill, NC 27599, USA. [5]Humanitas Research Hospital, Rozzano, MI 20089, Italy.
*Corresponding author. Email: wei.yang@duke.edu (W.Y.); luis.ulloa@duke.edu (L.U.)
†Present address: Autonomic Dysfunction Center, Vanderbilt University Medical Center, Nashville, TN 37232, USA.

reduced Ubc9 abundance in colonic endoscopic biopsies of patients with IBD, and specific *Ubc9* knockdown in human epithelial cells inhibited master kinase Akt1 SUMOylation and resulted in increased inflammation (*24*). However, SUMOylation is a complex mechanism with three main SUMO isoforms expressed in multiple cell types that play different roles in IBD (*24*, *28*–*31*). Here, we analyze the autonomic dysfunction induced by stress, its effects on acute colitis induced by dextran sulfate sodium (DSS), and whether electric stimulation of the cervical vagus nerve before the induction of colitis could improve colitis progression by regulating SUMOylation and reprogramming immune responses.

RESULTS

Vagal stimulation ameliorates stress-induced autonomic dysfunction and reduces colitis-related mortality in mice

Restraint stress induced by restraining the mice 6 hours daily for 21 days increased susceptibility to DSS colitis induction after the restraint period and turned colitis lethal, with all mice dead by day 5 after the challenge (Fig. 1A). There were no differences in body weights between the groups; however, stressed mice experienced more severe disease as measured by the multivariable colitis disease activity index (DAI) (Fig. 1B), mainly related to intestinal bleeding and stool consistency measures. Given that death prevented statistical

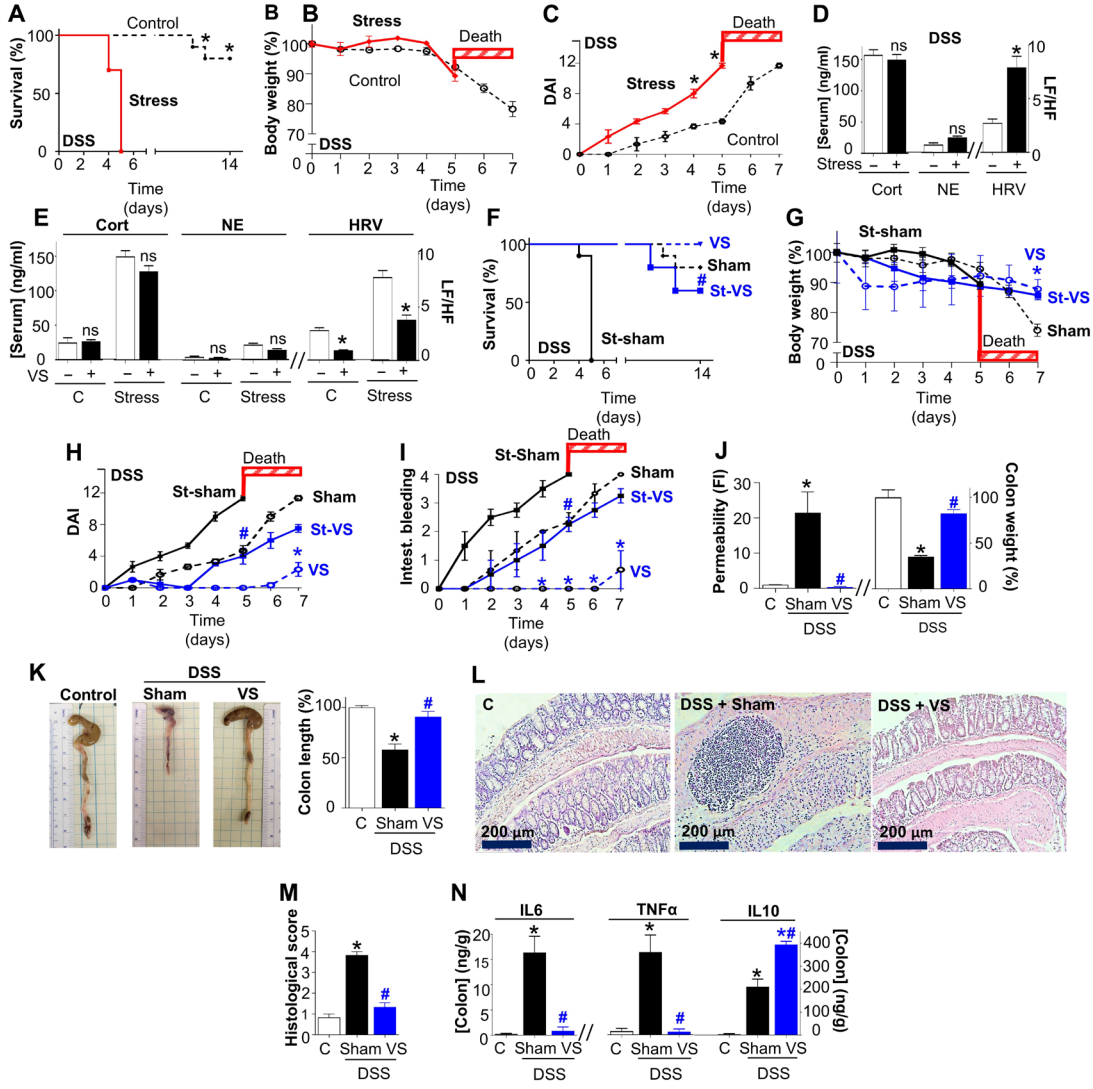

Fig. 1. Vagal stimulation improves outcomes in a mouse model of colitis. (**A**) Kaplan Meier survival curve and time course of (**B**) body weight and (**C**) DAI, (**D**) serum concentrations of corticosterone (Cort) or norepinephrine (NE), and HRV (measured as the LF/HF ratio) in 3% DSS mice with or without stress or (**E**) stressed and non-stressed mice with sham or vagal stimulation (VS). Stressed mice were subjected to 21 days of restraint then received either sham or VS followed by either clean water (control) or 5 days of DSS treatment. (**F**) Kaplan Meier survival curve and time course of (**G**) body weight, (**H**) DAI, and (**I**) intestinal bleeding in nonstress (dashed lines) and stress (solid lines, St) with and without sham or VS in stressed DSS mice with sham or VS. (**J**) Intestinal permeability, colon weights, (**K**) representative macroscopic colons and group colon lengths, (**L**) colonic hematoxylin and eosin (H&E; 20×; scale bars, 200 µm), (**M**) histological score, and (**N**) colon IL-6, TNF-α, and IL-10 concentrations at day 7 in control and DSS mice with sham or VS. Data are representative of experiments that were replicated on different dates. For survival analysis, mice were followed for 14 days; *$P < 0.05$ versus sham, #$P < 0.05$ versus St-sham DSS ($n = 10$ from two repeated experiments, log-rank test), *$P < 0.05$ versus control ($n = 5$, two-way ANOVA with Bonferroni's post hoc test), *$P < 0.05$ versus control, and #$P < 0.05$ versus sham DSS ($n = 5$, one-way ANOVA with Bonferroni's post hoc test). Graphs represent the mean ± SEM of experiments repeated twice on different dates.

group comparison at day 7 after DSS challenge, we indicated the time of death and monitored DAI in control mice to show the disease progression time course (Fig. 1C). To determine whether DSS concentration influences the susceptibility of mice to colitis, we tested 3 and 5% concentrations in nonstressed mice. We found no difference between DSS 3 and 5% in terms of stool consistency, intestinal bleeding, body weight loss, or DAI, nor did we see any difference with colon weight and length, organ adhesion, intestinal permeability, and colon cytokines between the two groups (fig. S1, A to H). Then, we analyzed the three major networks of neuromodulation in stressed and control mice; hypothalamic-pituitary-adrenal (HPA), sympathetic, and cardio-vagal networks, at day 5 after DSS challenge before the time point when the stressed mice are expected to die. We found no significant differences in plasma corticosterone concentrations (a marker of HPA axis) or norepinephrine (a marker for sympathetic adrenal axis). However, there was a threefold increase in the low frequency/high frequency (LF/HF) ratio, a measure of heart rate variability (HRV) and parasympathetic tone through the cardio-vagal axis (Fig. 1D). Because high LF/HF may reflect a parasympathetic deficiency, we analyzed whether electrical stimulation of the parasympathetic vagus nerve could compensate for these effects and improve colitis outcomes (*32*). Acute electric stimulation of the cervical vagus nerve (5 V, 50 Hz, 100 ms) for 15 min decreased the LF/HF ratio without affecting corticosterone or epinephrine concentrations compared to sham mice, which were subjected to the same surgical procedure without vagal stimulation (Fig. 1E). A control group of nonstressed mice was tested parallel to the sham group, and we did not observe any significant difference between the sham and control groups. Vagal stimulation could rescue stressed mice from DSS colitis–induced lethality and significantly improve DAI score and intestinal bleeding without a significant change in body weight loss (Fig. 1, F to I). These results are consistent with the literature showing that stool consistency and intestinal bleeding/permeability are the first symptoms as reflected in early DAI scores before body weight changes are noticeable, normally after day 5 of DSS treatment (*33*). Vagal stimulation also rescued normal mice (without stress) and prevented colitis-induced intestinal bleeding, DAI, body weight loss, and intestinal permeability (Fig. 1, F to J). Vagal stimulation preserved macroscopic and microscopic intestinal integrity (Fig. 1, K to M), reduced inflammatory cytokines interleukin-6 (IL-6) and tumor necrosis factor–α (TNF-α), and increased the anti-inflammatory cytokine IL-10 (Fig. 1N). Because these results suggested that vagal stimulation may improve colitis by inducing IL-10, we studied colitis and vagal stimulation in *IL10*-KO mice. *IL10*-KO mice were highly susceptible to DSS colitis, with early progression of DAI (Fig. 2A) and intestinal bleeding within the

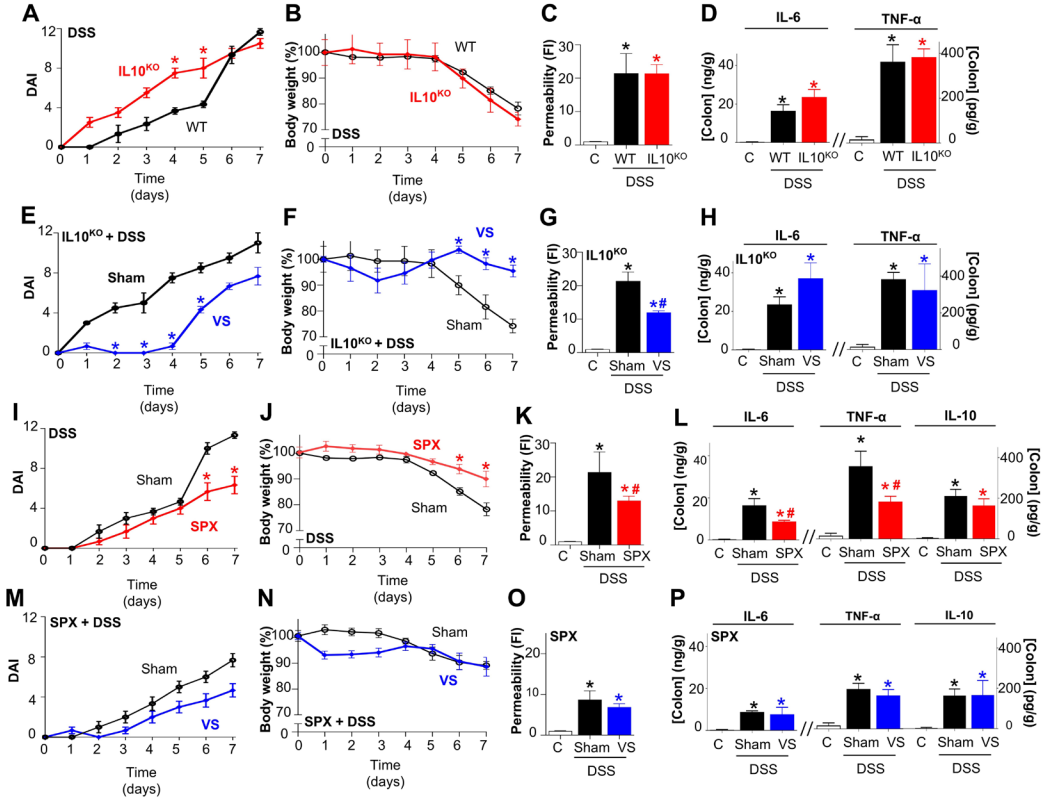

Fig. 2. Vagal regulation of colitis in mice is IL-10 independent and mediated by the spleen. Time course of (**A**) DAI, (**B**) body weight, (**C**) intestinal permeability, and (**D**) colon IL-6 and TNF-α concentrations in [(A) to (D)] *IL10*-KO (*IL10*^{KO}) mice and their wild-type (WT) littermates at day 7 after 5-day DSS challenge. Time course of (**E**) DAI, (**F**) body weight, (**G**) intestinal permeability, and (**H**) colon IL-6 and TNF-α concentrations in [(E) to (H)] *IL10*^{KO} at day 7 after receiving sham or VS immediately followed by 5-day DSS challenge. Time course of (**I**) DAI, (**J**) body weight, (**K**) intestinal permeability, and (**L**) colon IL-6, TNF-α, and IL-10 concentrations in [(I) to (L)] splenectomized (SPX) or sham mice at day 7 after 5-day DSS challenge. Mice were SPX 5 days before the DSS, sham, or VS treatment. Time course of (**M**) DAI, (**N**) body weight, (**O**) intestinal permeability, and (**P**) colon IL-6, TNF-α, and IL-10 concentrations in [(M) to (P)] SPX at day 7 after receiving sham or VS immediately followed by 5-day DSS challenge. *$P < 0.05$ versus control and #$P < 0.05$ versus DSS ($n = 5$, one-way ANOVA with Bonferroni's post hoc test). Graphs represent the mean ± SEM of experiments repeated twice on different dates.

first 24 hours (fig. S2, A and B). Wild-type and *IL10*-KO mice had similar body weight loss (Fig. 2B), colon permeability, colon length, organ adhesion, and inflammatory cytokine concentrations at euthanasia on day 7 (Fig. 2, C and D; and fig. S2C). Vagal stimulation protected *IL10*-KO mice from onset of colitis until after the first 4 days and reduced body weight loss, intestinal permeability, stool consistency, and intestinal bleeding with nonsignificant alteration of IL-6 or TNF-α concentrations by euthanasia at day 7 (Fig. 2, E to H; and fig. S2, D to F). These results suggested that vagal protection against colitis was largely independent of IL-10.

Splenectomy blocks vagal protection against colitis in mice

The mechanism of vagal regulation of colitis is unknown because most of the colon lacks efferent vagal innervation. We have previously reported that the spleen is a critical link between the nervous and immune systems that regulates innate immune responses to bacterial challenge in endotoxemia (*16*, *34*, *35*), and so we postulated that the spleen may also contribute to vagal regulation of colitis. Surgical splenectomy followed by initiation of colitis by administration of DSS 5 days later resulted in little change to early stool consistency, intestinal bleeding, colon length, and organ adhesion, but improved DAI scores after day 5 (Fig. 2I and fig. S3, A to C). Splenectomy before onset of colitis led to improved colon integrity, body weight, and intestinal permeability, and reduced colon IL-6 and TNF-α concentration, without affecting IL-10 concentrations (Fig. 2, J to L). Moreover, splenectomy blocked the protective effects of vagal stimulation in DAI score, colon length, permeability, cytokine concentrations, stool consistency, intestinal bleeding, colon length, and organ adhesion (Fig. 2, M to P; and fig. S3, D to F).

Vagal stimulation is partially dependent on α7-nicotinic acetylcholine receptors (α7nAChRs) in controlling colitis

We and others have reported that vagal stimulation controls inflammation in endotoxemia by inhibiting macrophages via α7-nicotinic acetylcholine receptors (α7nAChRs) (*17*, *36*–*38*). We therefore analyzed whether α7nAChRs contribute to the vagal regulation of colitis. *Chrna7*-KO colitis mice had lower DAI scores and experienced less body weight loss and intestinal permeability with no difference in macroscopic images, colon length, and weight compared to wild-type colitis mice, similar to that seen in splenectomized mice (Fig. 3, A and B to E). In addition, there were no differences in stool consistency, intestinal bleeding, and organ adhesion between *Chrna7*-KO

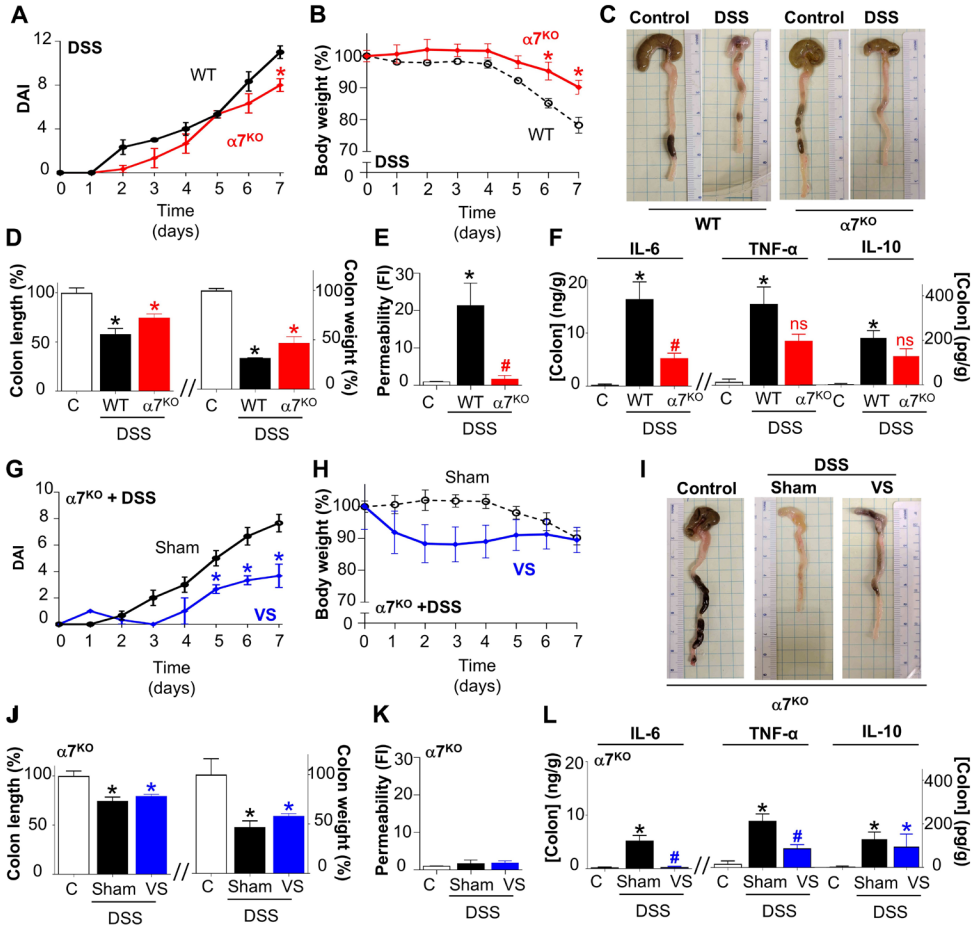

Fig. 3. Vagal protection against colitis is partially dependent on α7nAChR. Time course of (**A**) DAI, (**B**) body weight, and (**C**) representative colons, (**D**) group colon lengths and weight, (**E**) intestinal permeability, and (**F**) colon immune cytokines in [(A) to (F)] *Chrna7*-KO ($\alpha7^{KO}$) or WT littermates at day 7 after 5-day DSS challenge. Time course of (**G**) DAI, (**H**) body weight, and (**I**) representative colons, (**J**) group colon lengths and weight, (**K**) intestinal permeability, and (**L**) colon immune cytokines in [(G) to (L)] *Chrna7*-KO ($\alpha7^{KO}$) mice at day 7 after receiving sham or VS immediately followed by 5-day DSS challenge. *$P < 0.05$ versus control and #$P < 0.05$ versus WT or DSS ($n = 4$, one-way ANOVA with Bonferroni's post hoc test). Graphs represent the mean ± SEM of experiments repeated twice on different dates.

and wild-type colitis mice (fig. S4, A to C) *Chrna7*-KO colitis mice had lower IL-6 but similar TNF-α and IL-10 concentrations in the colon compared to wild-type mice with colitis (Fig. 3F). Vagal stimulation improved DAI scores and stool consistency after day 4 in *Chrna7*-KO mice (Fig. 3G and fig. S4D). Although we did not detect a significant effect on body weight loss, intestinal permeability, intestinal bleeding, organ adhesion, macroscopic images, colon weight, and colon length, vagal stimulation reduced IL-6 and TNF-α but not IL-10 concentrations in the colons of *Chrna7*-KO colitis mice on day 7 (Fig. 3, H to L; and fig. S4, E and F). These results suggest that vagal stimulation may induce two protective mechanisms, one dependent on α7nAChRs to induce IL-10 and partially inhibit TNF-α and a second α7nAChR-independent mechanism to inhibit IL-6 and TNF-α.

Acetylcholine is the principal neurotransmitter of the vagus nerve and signals through nicotinic receptors. Given the known protective effects of nicotine on UC (*39*, *40*), we assessed whether nicotine could replicate vagal neuromodulation of colitis. Treatment with nicotine was less effective than vagal stimulation and did not improve DAI scores during the first 4 days of treatment, but it did reduce intestinal bleeding and body weight loss on days 6 and 7, although the effects were minor (Fig. 4, A to C). By euthanasia on day 7, nicotine substantially reduced intestinal permeability and IL-6 and TNF-α concentrations, without affecting IL-10 (Fig. 4, D and E). Next, we analyzed whether the effects of nicotine were mediated by α7nAChR using *Chrna7*-KO mice. Nicotine did not improve DAI scores, intestinal bleeding, body weights, colon length, or intestinal permeability in *Chrna7*-KO mice (Fig. 4, F to I). However, nicotine did inhibit IL-6 and TNF-α concentrations in the colons of *Chrna7*-KO mice (Fig. 4J). These results suggest that nicotine can protect reduce inflammatory cytokines in colitis through a mechanism independent of α7nAChRs.

SUMOylation is a dynamic regulatory process in human IBD and vagal neuromodulation

We recently reported that SUMOylation helps orchestrate immune responses to bacterial infection (*23*, *41*, *42*). Thus, we first analyzed Ubc9 transcripts in our mRNA databank of human biopsy samples where single-cell sequencing data are available under Gene Expression Omnibus (GEO) accession GSE164985 (*43*–*46*). There was no statistically significant difference between the *Ubc9* transcripts from

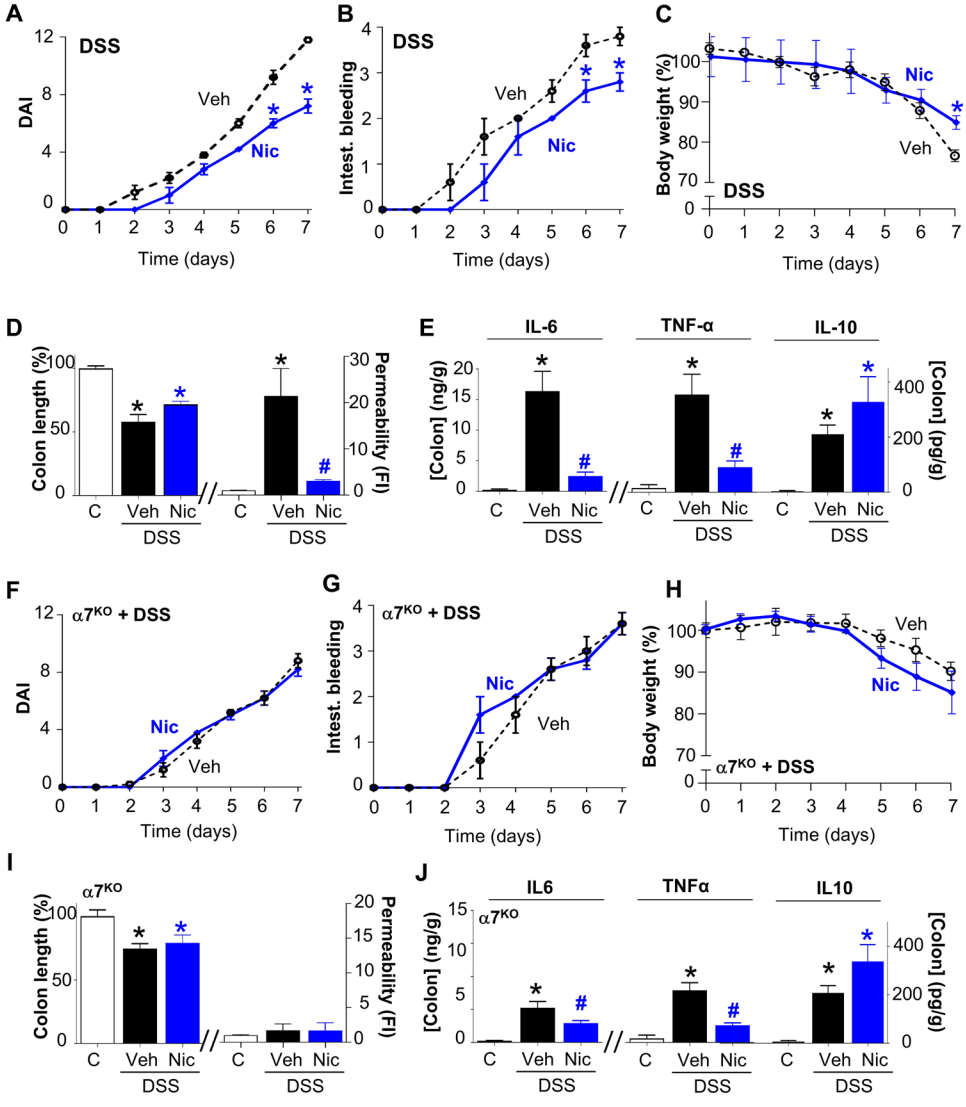

Fig. 4. Nicotine improves colitis outcomes in mice through α7nAChRs. Time course of (**A**) DAI, (**B**) intestinal bleeding, (**C**) body weight, (**D**) colon length, intestinal permeability, and (**E**) colon immune cytokines in [(A) to (E)] WT mice at day 7 after 5-day DSS challenge with 3-day nicotine (Nic) treatment or vehicle (veh). Time course of (**F**) DAI, (**G**) intestinal bleeding, and (**H**) body weight, and (**I**) colon length, intestinal permeability, and (**J**) colon immune cytokines in [(F) to (J)] *Chrna7*-KO ($\alpha7^{KO}$) mice at day 7 after 5-day DSS challenge with 3-day nicotine treatment or vehicle. *$P < 0.05$ versus control and #$P < 0.05$ versus DSS ($n = 5$, one-way ANOVA with Bonferroni's post hoc test). Graphs represent the mean ± SEM of experiments repeated twice on different dates.

91 patients with CD and 29 non-IBD controls ($P = 0.34$, Fig. 5A). There are three SUMO isoforms, termed SUMO1, SUMO2, and SUMO3, with SUMO2 and SUMO3 referred to together as SUMO2/3 because of their homology. We collected 18 human samples from intestinal biopsies and surgical resections from the ascending colons of nine healthy controls without IBD, two patients with UC, and seven patients with CD to analyze SUMOylation via Western blot and immunohistochemistry. Western blotting did not reveal major changes in SUMO1 but did show a strong increase in SUMO2/3 abundance in samples from patients with CD as shown by the high molecular "smear" representative of SUMOylation of multiple proteins as compared with patients who did not have IBD (Fig. 5B). Immunohistochemistry analyses of human biopsies also demonstrated stronger SUMO2/3 staining in samples from patients with CD (Fig. 5C). Western blots of colon samples from wild-type mice with DSS-induced colitis showed similar patterns of SUMOylation without major changes in SUMO1 but about twofold increases in SUMO2/3 smear ≈250 kDa (Fig. 5D). Immunohistochemistry analyses also demonstrated a stronger and broader distribution of SUMO2/3 in the colons of colitis mice (Fig. 5E). Vagal stimulation decreased SUMO1 by nearly 30% and SUMO2/3 by 70% compared with sham colitis mice (Fig. 5, D and E).

SUMO isoforms regulate different stages of colitis in mice

We next analyzed the specific roles of different SUMO isoforms in colitis and vagal neuromodulation using global *Sumo1*-KO and *Sumo3*-KO mice (*47*, *48*). *Sumo2*-KO mice were not analyzed because embryos die during early development (*47*, *48*). *Sumo1*-KO DAI scores plateaued on day 3, and mice were thereafter resistant to the progression of colitis (Fig. 6A and fig. S5, A to C). By contrast, *Sumo3*-KO mice were resistant to colitis during the first 5 days (Fig. 6A and fig. S5, A to C). Both *Sumo1*-KO and *Sumo3*-KO mice were more resistant to intestinal permeability and had lower IL-6 and TNF-α colon concentrations on day 7 than wild-type mice (Fig. 6, B to D). Vagal stimulation protected *Sumo1*-KO mice against colitis through day 4 as shown by the lower DAI and body weight loss but similar colon length, intestinal permeability, colon IL-6, and TNF-α as well as higher IL-10 compared with sham *Sumo1*-KO mice (Fig. 6, E to H). Similarly, vagal stimulation improved stool consistency and intestinal bleeding through day 4 and reduced colon shortening and organ adhesion at day 7 in *Sumo1*-KO mice (fig. S5, D to F). By contrast, vagal stimulation improved DAI scores in *Sumo3*-KO mice after day 5 (Fig. 6I and fig.S5, G to I). Vagal stimulation prevented intestinal permeability in *Sumo1*-KO and *Sumo3*-KO mice by 65 and 35%, respectively (Fig. 6, G and K). By day 7, vagal stimulation increased IL-10 concentrations in both *Sumo1*-KO and *Sumo3*-KO mice by nearly fourfold (Fig. 6, H and J). The protection of *Sumo1*-KO mice after day 3 correlates with the timing of immune cell influx into the mouse intestine during DSS-induced colitis (*49*, *50*) and prompted us to ask whether the protection induced by SUMO1 depletion may be due to immune cells. We therefore performed bone marrow transplants from wild-type, *Sumo1*-KO, and *Sumo3*-KO mice into irradiated wild-type mice. Mice received lethal dose of x-ray irradiation followed by bone marrow rescue 5 hours later and were monitored for 4 weeks until complete donor chimerism was seen, then we started DSS treatment. The transfer of wild-type and *Sumo3*-KO bone marrow resulted in increased DAI scores, body weight loss, intestinal permeability, and immune responses in irradiated wild-type mice (Fig. 6, M to P). However, the transfer of *Sumo1*-KO bone marrow significantly protected irradiated wild-type mice against increases in DAI, body weight loss, intestinal

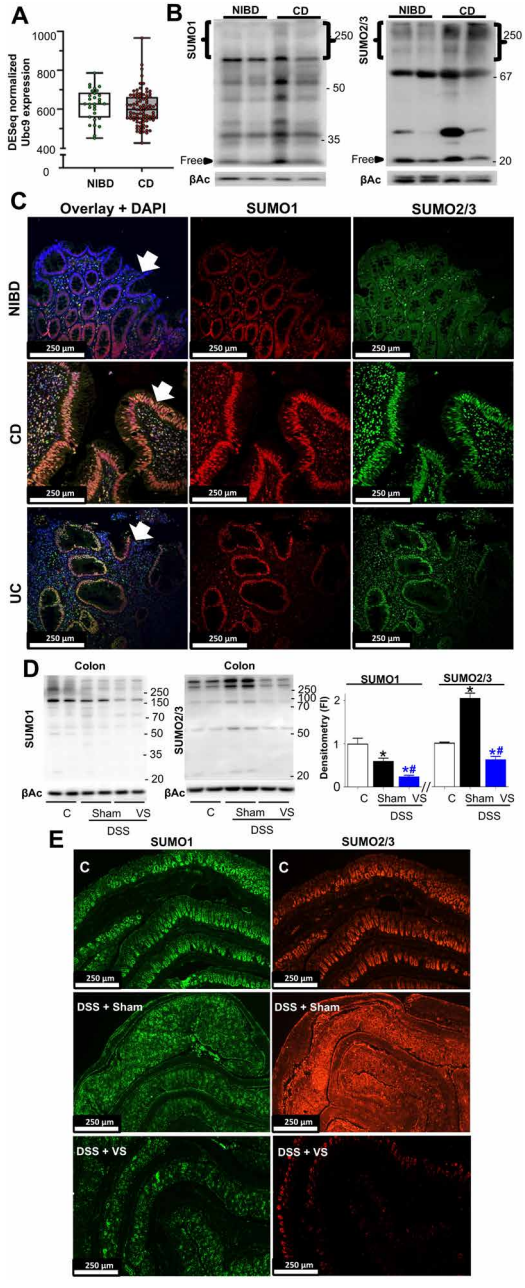

Fig. 5. SUMOylation in human biopsy and vagal regulation of colitis. (**A**) DEseq normalized counts for *Ubc9* expression in human biopsy samples from 29 patients without IBD (NIBD) and 91 patients with CD ($P = 0.34$). Single-cell sequencing data are available under GEO accession GSE164985. (**B**) Western blots and (**C**) representative immunohistochemistry (IHC) for SUMO1 (red, center column) and SUMO2/3 (green, right column) of colon biopsy from NIBD (top row) and patients with UC (middle row) and CD (bottom row). Merged images are shown in the left column (nuclei were stained blue with DAPI). Data show representative results of seven biopsies from 18 human samples analyzed. Brackets in (B) point to the typical high–molecular weight smears induced by SUMOylation. (**D**) Western blots, densitometric analyses, and (**E**) representative IHC for SUMO1 and SUMO2/3 of colon samples from control or 3% DSS mice with sham or VS. White scale bars are equivalent to 250 μm, whereas arrows point to intestinal crypt epithelium. Western blots represent experiments repeated at least twice on different days, and graphs show mean ± SEM of fold of induction (FI). *$P < 0.05$ versus control and #$P < 0.05$ versus DSS ($n = 5$ per group, two-way ANOVA with Tukey's post hoc test).

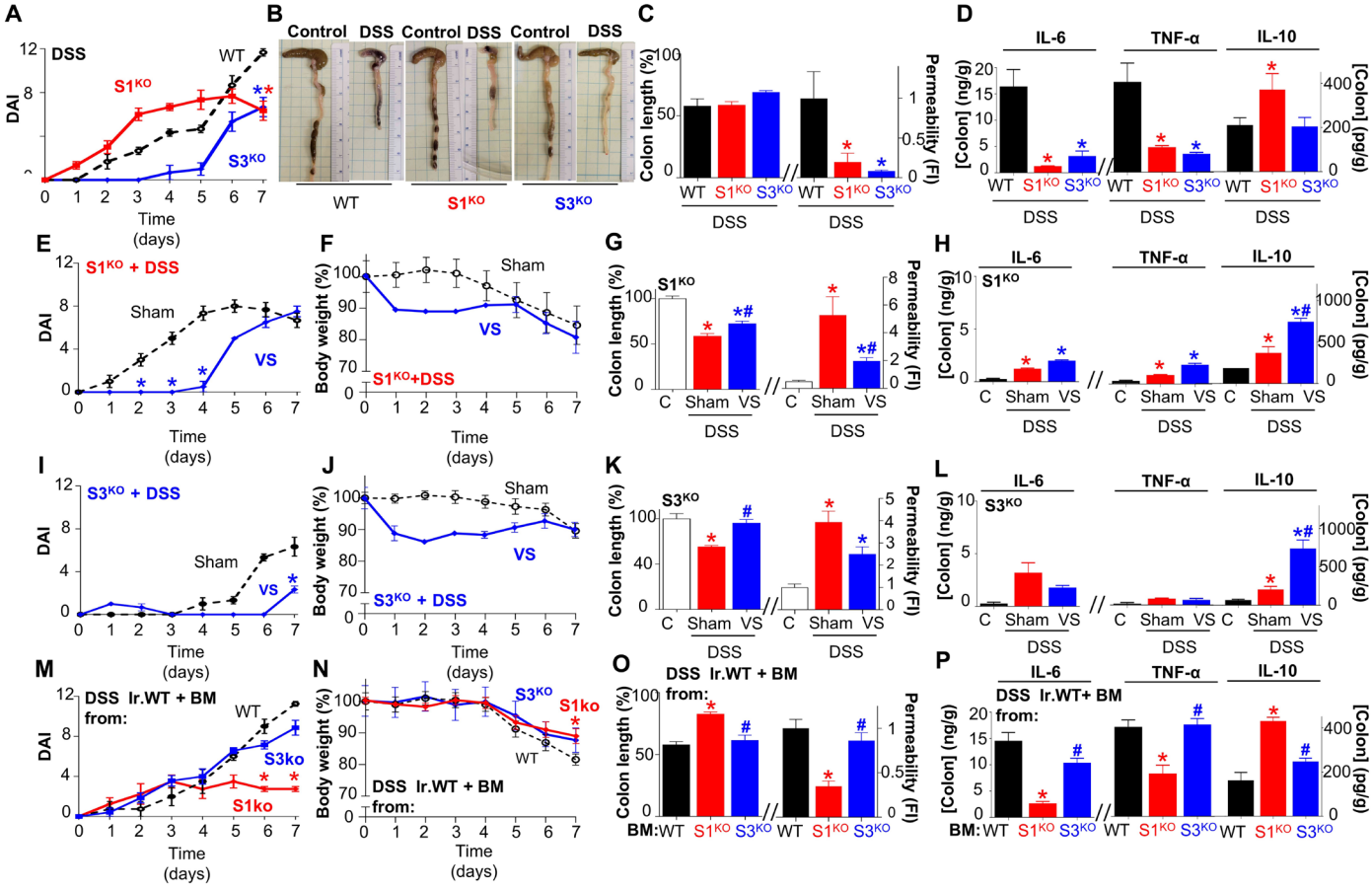

Fig. 6. Bone marrow transfer from *Sumo1*-KO mice confers protection against colitis. (**A**) DAI, (**B**) representative colons, (**C**) group colon lengths and intestinal permeability, and (**D**) immune cytokines in [(A) to (D)] *Sumo1*-KO, *Sumo3*-KO, and their wild-type littermate controls at day 7 after 5-day DSS challenge. (**E**) DAI, (**F**) body weight, (**G**) group colon lengths and intestinal permeability, and (**H**) immune cytokines in [(E) to (H)] *Sumo1*-KO at day 7 after receiving sham or VS immediately followed by 5-day DSS challenge. (**I**) DAI, (**J**) body weight, (**K**) group colon lengths and intestinal permeability, and (**L**) immune cytokines in [(I) to (L)] *Sumo3*-KO at day 7 after receiving sham or VS immediately followed by 5-day DSS challenge. (**M**) DAI, (**N**) body weight, (**O**) group colon lengths and intestinal permeability, and (**P**) immune cytokines in [(M) to (O)] irradiated wild-type DSS (Ir.WT + BM) mice transferred with wild-type, *Sumo1*-KO, or *Sumo3*-KO bone marrow and received 5-day DSS challenge starting at day 28 after bone marrow transplantation and assessed at day 7 after DSS challenge. **P* < 0.05 versus control or WT and #*P* < 0.05 versus DSS (*n* = 4, one-way ANOVA with Bonferroni's post hoc test). Graphs represent the mean ± SEM of experiments repeated twice on different dates.

permeability, and inflammatory responses while increasing colon IL-10 concentrations by nearly threefold. These results revealed the differences between SUMO1 and SUMO3 in the pathogenesis and progression of colitis and suggested that vagal stimulation protects against colitis by inhibiting SUMOylation.

Inhibition of SUMOylation with TAK-981 rescued mice from established colitis

Because vagal stimulation is an invasive surgical procedure, we next tested whether pharmacological inhibition of SUMOylation mimics vagal stimulation and protects against colitis. We used TAK-981 (subasumstat), a first-in-class inhibitor of the transfer of SUMO to Ubc9 (*43*–*45*, *51*). First, we confirmed that TAK-981 inhibits both SUMO1 and SUMO2/3 in the colons of DSS mice (fig. S6, A to D). The efficacy of TAK-981 treatment was also confirmed using Western blotting against negative control samples from knockout mice to ensure successful inhibition of SUMOylation (fig. S6, A to F). Because previous studies reported that bacterial endotoxin induces SUMOylation (*23*), we also confirmed that TAK-981 inhibits SUMOylation in the spleens of endotoxemic mice (fig. S6, C and D). The specificity of the staining was confirmed in extracts from *Sumo1*-KO and *Sumo3*-KO mice. Mice were treated with TAK-981 (7.5 mg/kg) 12 hours before the start of DSS challenge and then daily for 4 days. TAK-981 protected against colitis, improved DAI scores, preserved the macroscopic and histological integrity of the colon, prevented body weight loss, and almost reduced intestinal permeability by nearly 90% (Fig. 7, A to E). TAK-981 reduced colon IL-6 and TNF-α concentrations by 80 and 65%, respectively, without affecting IL-10 concentrations (Fig. 7F).

We next analyzed whether TAK-981 treatment can rescue mice from established colitis. TAK-981 treatment, starting 3 days after the DSS challenge, ameliorated colitis and improved DAI scores by reducing intestinal bleeding and body weight loss (Fig. 8, A to C). TAK-981 also improved DAI scores, intestinal bleeding, and body weights in experimental CD induced by TNBS (2,4,6-trinitrobenzene sulfonic acid, Fig. 8, D to F). These results prompted us to hypothesize that TAK-981 might preserve intestinal integrity and inhibit colitis progression to sepsis, a potentially lethal complication in patients with

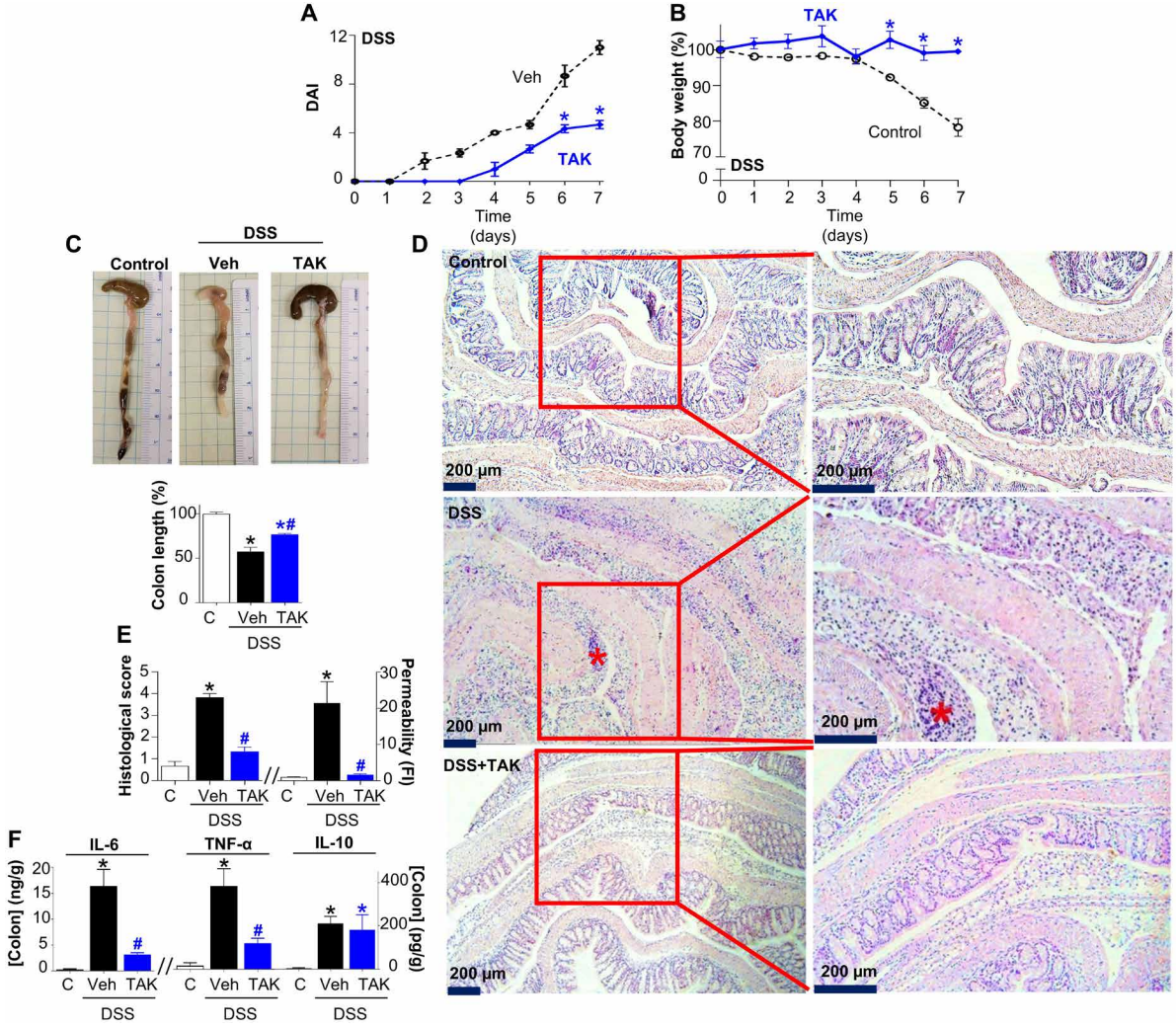

Fig. 7. Inhibition of SUMOylation with TAK-981 improves colitis outcomes in mice. (**A**) DAI, (**B**) body weight, (**C**) representative colons and group colon lengths, (**D**) H&E of colonic tissues (10×, 20×; scale bars, 200 μm), (**E**) histological score, intestinal permeability, and (**F**) colon immune cytokines in control or colitis mice treated with vehicle or TAK-981 at day 7 after 5-day DSS challenge. Mice were treated with TAK-981 (7.5 mg/kg) 12 hours before starting DSS challenge and then daily for 4 days. *$P < 0.05$ versus control and #$P < 0.05$ versus DSS ($n = 5$, one-way ANOVA with Bonferroni's post hoc test).

IBD. Thus, we used TAK-981 to treat mice with oxazolone-induced colitis, an experimental model of severe UC associated with mucosal damage that can progress to sepsis (*52*, *53*). TAK-981 treatment started before oxazolone challenge improved DAI scores, reduced intestinal bleeding and body weight loss, and improved intestinal integrity (Fig. 8, G to K). TAK-981 treatment also reduced intestinal permeability and peritoneal bacterial leakage by nearly 90% (Fig. 8L) and IL-6 and TNF-α by nearly 70% without substantially affecting IL-10 (Fig. 8M). Together, these results demonstrated that inhibition of SUMOylation with TAK-981 during colitis might prove advantageous for treating patients with IBD.

DISCUSSION

Epidemiological studies have suggested an association between stress and IBD relapses, regardless of whether stress is consciously perceived (*54*). Our results showed that stress results in lethal colitis within 5 days after the DSS challenge. We selected stress induced by physical restraint, without constraint or pain, to avoid circadian or metabolic dysfunction induced by other models such as sleep or food deprivation (*55*, *56*). Stress induced a higher LF/HF ratio in HRV frequency analyses, suggesting parasympathetic dysfunction. We previously reported that vagal dysfunction contributes to inflammatory disorders and that vagal stimulation can curb inflammatory responses to bacterial endotoxin (*34*, *35*). Considering the previous studies reporting that stress can affect immune responses in mice via C1 neurons (*57*), it is possible that the abrogation of stress-induced immune dysfunction is one mechanism of vagal anti-inflammatory effects. The mechanism of vagal regulation of colitis is unknown and likely complex because the colon lacks efferent vagal innervations. Thus, previous studies focused on experimental CD induced by TNBS in the small intestine rather than colitis. Two recent studies reported that prophylactic chronic vagal stimulation can improve outcomes in rats with TNBS-induced colitis (*58*, *59*). These studies are limited by the variability of colon inflammation in IBD experimental models using haptenizing agents like TNBS or oxazolone

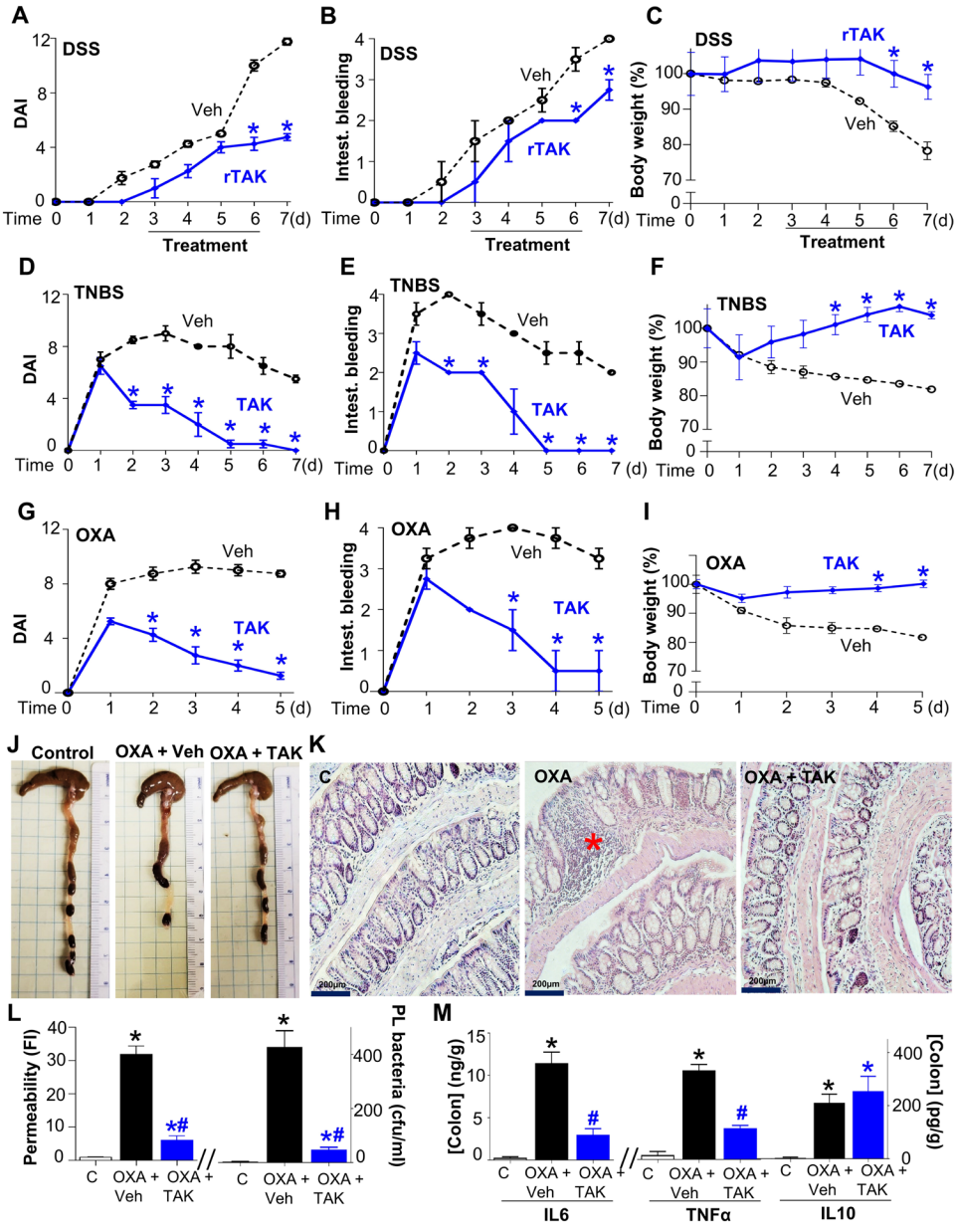

Fig. 8. TAK-981 treatment ameliorates disease in three mouse models of IBD. (**A**) DAI, (**B**) intestinal bleeding, and (**C**) body weight at day 7 of 5-day DSS challenge in mice treated with vehicle or rescue TAK-981 (rTAK) started at day 3 after DSS and daily for 4 days. (**D**) DAI, (**E**) intestinal bleeding, and (**F**) body weight at day 7 of TNBS (150 mg/kg) rectal instillation in mice treated with vehicle or TAK-981 started 12 hours before TNBS challenge and daily for 4 days. (**G**) DAI, (**H**) intestinal bleeding, (**I**) body weight, (**J**) representative macroscopic images, (**K**) microscopic images, (**L**) intestinal permeability, peritoneal lavage bacteria, and (**M**) colon inflammatory cytokines at day 5 of oxazolone (1%) (OXA) rectal instillation in mice treated with vehicle or TAK-981 started 12 hours before oxazolone challenge and daily for 4 days. **P* < 0.05 versus vehicle (*n* = 4, two-way ANOVA with Bonferroni's post hoc test), **P* < 0.05 versus control, and #*P* < 0.05 versus OXA (*n* = 4, one-way ANOVA with Bonferroni's post hoc test).

(*59*). Despite its invasiveness, vagal stimulation in IBD mouse models is a very efficient tool to study local and systemic immune regulation and define new molecular targets for future drug discovery.

Our results concur with clinical studies showing that therapies increasing cardiovagal activity, such as mind-body interventions, alleviate IBD symptoms, but their clinical use is hampered by limited efficacy. Vagal stimulation protected mice from colitis for the first 5 days after DSS exposure. Stool consistency and intestinal bleeding and permeability are generally the first signs of mucosal barrier injury before body weight changes are noticeable around day 5 of DSS treatment. These results prompted us to analyze the local and systemic vagal mechanisms of neuromodulation mediated by the spleen.

The vagal induction of IL-10 concurs with the high susceptibility of *IL10*-KO mice to colitis. IL-10–deficient mice have normal lymphocyte development and antibody responses but are anemic and develop chronic enterocolitis (*60*). Vagal stimulation protected *IL10*-KO mice from colitis, revealing an IL-10–independent mechanism. We have previously reported that the spleen is a critical link between the nervous and immune systems in endotoxemia (*16*, *61*). Vagal stimulation activates the "cholinergic anti-inflammatory pathway," curbing unfettered inflammation in experimental sepsis by inhibiting the production of inflammatory cytokines in splenic macrophages via α7nAChRs (*62*–*64*). We now report that splenectomy prevented vagal regulation of colitis. These results were also consistent with recent clinical studies showing splenomegaly (*65*) with splenic abscesses as an early manifestation of CD (*66*) and dysfunctional hypersplenism with higher pitted erythrocyte counts in patients with relapsed UC (*67*). These results suggested that the spleen may be a therapeutic target for neuromodulation and bioelectronic strategies. We also noted that vagal stimulation protected *Chrna7*-KO

mice against DSS colitis. Because vagal stimulation failed to control systemic inflammation in *Chrna7*-KO mice in endotoxemia, this suggests a mechanism of vagal neuromodulation in colitis independent of the canonical vagal IL-10/α7nAChR vagal pathway. Future physiological and cellular studies will be required to delineate this complex vagal-immune neuronal network, as well as the specific cells regulated in the spleen and colon.

SUMOylation is emerging as a stress-adaptive response to safeguard intestinal integrity, a tissue particularly challenged by its bacterial environment (*23*, *24*, *28*–*31*, *42*). A previous study reported lower Ubc9 expression in colonic biopsy samples from patients with UC and CD ($n = 22$ per group) (*24*). We did not find a significant difference in *Ubc9* expression between samples from 91 patients with CD and 29 non-IBD controls ($P = 0.34$). This lack of difference may be due to patient selection, with a wide range of ages and disease activity. Western blot and immunohistochemistry revealed an increase of SUMO2/3 but not SUMO1 in human samples and murine models. *Sumo1*-KO mice were resistant to colitis progression, whereas *Sumo3*-KO mice were resistant to the early stages of colitis, and bone marrow transplants from *Sumo1*-KO but not *Sumo3*-KO mice, conferred protection to irradiated wild-type mice against colitis, demonstrating differences between the contributions of the SUMO1 and SUMO3 isoforms to colitis. The typical high–molecular weight smears observed in Western blots on samples from patients with CD and mouse models reflect SUMOylation of multiple proteins. SUMOylation controls multiple pathways and can target several proteins within the same pathway, such as asp65, inhibitor of nuclear factor κB, and centrobin-centrosomal protein 4.1–associated protein in the nuclear factor κβ pathway (*68*–*70*). Future in vivo and in vitro studies will be required to define the specific targets of SUMO1 and SUMO3 in splenic and colonic cells during colitis.

Our study has several limitations. First, it is unclear which part of the vagus nerve plays a dominant role in IBD regulation. We have recently used an afferent vagal stimulation model to demonstrate the role of vagal sensory regulation in insulin secretion (*71*). Although this model was successful in improving short-term metabolic readouts, it involves cervical vagotomy, which shortens mouse survival, and implementation in colitis models would be technically difficult. Future studies of afferent vagal neuromodulation in colitis models with the help of optogenetics may be warranted. Another limitation of our study is the use of global *Sumo* KO models, which prevent delineation of the specific effector compartments of SUMO regulation in IBD. Although we started to tackle this problem using bone marrow transplant chimeras, the availability of conditional knockouts will help us to further elucidate the precise compartments in future studies. Another limitation of this study is the use of male mice only to limit variability in results. In addition, although we have shown the importance of cell trafficking for specific SUMO1 inhibition, it is still unclear whether this is mediated through decreased inflammatory cell influx or increased anti-inflammatory cell influx. Future flow cytometric studies are warranted to further understand the role of trafficking immune cells in conveying the anti-inflammatory properties of SUMO inhibition in IBD. Also, the mechanisms of local protective effects of SUMO3 inhibition in the gut are not yet fully understood.

Our results showed that SUMOylation is regulated by neuromodulation and that vagal stimulation can control SUMOylation in murine models of colitis. We then tested whether pharmacological inhibition of SUMOylation mimicked vagal stimulation and protected against colitis. Treatment with the SUMOylation inhibitor TAK-981 improved both DSS colitis and TNBS CD in mice. TAK-981 treatment also reduced intestinal permeability and bacterial leakage in oxazolone-induced colitis, an experimental model of severe UC associated with mucosal damage that can progress to sepsis (*52*, *53*). In conclusion, these results show that modulation of SUMOylation through vagal stimulation or treatment with a SUMOylation inhibitor can ameliorate colitis in mouse models, suggesting these approaches as potential therapies for patients with IBD.

MATERIALS AND METHODS

Study design

The aim of this study was to identify the role of vagal neuromodulation in murine colitis and to assess its pharmacologic translation via SUMO inhibition. Sample sizes were determined according to our previous studies and preliminary results. Sample sizes are included in the figure legends. Investigators were blinded to mouse treatment groups during DAI score assessment and histological assessments. Mice were randomized for control, vagal stimulation, or drug treatment.

Chemicals and reagents

DSS salt (molecular weight, 35 to 60 kDa; MP Biomedicals) was dissolved in autoclaved deionized water (*33*, *72*, *73*). TNBS (Sigma-Aldrich) was used at a single dose of 150 mg/kg (150 μl, rectally). 4-Ethoxymethylene-2-phenyl-2-oxazolin-5-one (oxazolone, Sigma-Aldrich) was used at 1% (w/v) in 50% ethanol (150 μl, rectally) 7 days after epicutaneous sensitization with 3% (w/v) oxazolone in ethanol. Nicotine was dissolved in autoclaved drinking water at 20 μg/ml (*74*). Mice were treated with nicotine 3 days before and daily for 5 days after DSS treatment as reported (*74*). TAK-981 (ChemieTek) (*43*–*45*, *51*) was dissolved in dimethyl sulfoxide (stock concentration, 50 mg/ml; stored at −20°C), diluted in pharmaceutical-grade corn oil (Sigma-Aldrich) at 7.5 mg/kg, and administered subcutaneously 12 hours before the start of colitis induction, then daily for 4 days as we reported (*23*).

Animal experiments

Animal procedures were approved by the Institutional Animal Care and Use Committee of Duke University. Six- to 8-week-old (~25 ± 5 g) male C57BL/6, male *Il10*-KO mice (*60*), and *Chrna7*-KO mice were obtained from Jackson Laboratory. *Sumo1*-KO, *Sumo3*-KO, and wild-type littermate mice were bred in our laboratory as previously described (*47*, *48*). Genotyping was performed by polymerase chain reaction (PCR) using tail genomic DNA and the Extract-N-Amp Tissue PCR kit (Sigma-Aldrich) (*47*, *48*). Mice were maintained on 12-hour light-dark cycle, with free access to food and water (ad libitum) and randomized into experimental groups; outcome assessors were blinded to group treatments.

Restraint stress

Stress was induced by restraining the mice for 6 hours daily for 3 weeks in well-ventilated polypropylene tubes without physical compression or pain described (*55*, *56*).

Heart rate variability

Three stainless steel electrodes were implanted in the right and left pectoral muscles and the abdominal wall using cardiac pacing wires (A & E Medical), then tunneled under the skin. The electrodes were exteriorized from the mouse nape and connected to MP150 research system (Biopac) for lead II electrocardiogram (EKG) recording.

Mice were allowed to recover for 5 days before recording the lead II EKG. AcqKnowledge software was used for HRV frequency domain analyses on the basis of the consecutive RR intervals of the 15-min EKG recordings. Low- and high-frequency domains were calculated, and the ratio was used as an indicator of the sympathetic-vagal balance as described (*58*).

Experimental IBD

DSS colitis

In the initial experiments (fig. S1, A to H), we used 3 and 5% DSS in autoclaved drinking water for 5 days as described in the literature (*33*). Thereafter, all experiments were performed with 3% DSS. For survival analysis, animals treated with DSS 3% were followed for 14 days to rule out delayed deaths.

TNBS colitis

Mice were fasted overnight and then given 150 μl of TNBS (150 mg/kg) in 50% ethanol injected intrarectally using a polyurethane P20 tube (Becton Dickinson) advanced gently 4 cm (from the anal verge) into the mouse rectum as previously described (*75*, *76*). The mice were held vertically for 1 min after injection to make sure that TNBS was retained in the rectum.

Oxazolone (4-ethoxymethylene-2-phenyl-2-oxazolin-5-one) colitis

A 2 cm–by–2 cm area of the abdomen was shaved, and mice were presensitized with the percutaneous application of 150 μl of 3% oxazolone w/v in 100% ethanol as previously described (*77*). Seven days later, mice received 150 μl of 1% oxazolone (w/v) in 50% ethanol intrarectally, then held vertically for 1 minute to ensure the retainment of oxazolone in the rectum.

In the three models of colitis, body weight, stool consistency, blood in stools by Hemoccult test (Hemoccult Sensa, Beckman Coulter) and water consumption were recorded daily during the experiment to calculate DAI score (*78*). Intestinal permeability was analyzed with oral gavage of fluorescein isothiocyanate dextran [0.6 mg/g body weight in phosphate-buffered saline (PBS)] 3 hours before terminal blood collection (*79*). Mice were euthanized on the indicated day, blood was collected by cardiac puncture, and intestines were collected for further analysis.

Disease activity index

DAI was recorded daily, assessing the preclinical parameters as described (*78*). Weight loss was scored (compared with baseline weight): 0, no loss or weight gain; 1, 5 to 10%; 2, 10 to 15%; 3, 15 to 20%; and 4, >20% loss from baseline weight. Stool consistency was scored: 0, well-formed stools; 1, sticky stools; 2, soft stools; 3, semi-solid loose stools; and 4, watery diarrhea. Rectal bleeding was scored: 0, no bleeding; 2, occult blood (by Hemoccult Sensa, Beckman Coulter); 3, bloody stools; and 4, gross rectal bleeding. Mice were immediately euthanized if they lost more than 20% of their baseline body weight.

Vagal stimulation

Mice were anesthetized using 3 to 5% isoflurane, intubated, and connected to a ventilator to allow 45 to 55 ml/min airflow with 30% oxygen and 1 to 2% maintenance isoflurane as we described (*80*). EKG leads were attached to the right and left forelimbs and hindlimbs to monitor heart rate. The front of the neck was shaved and sterilized (70% ethanol and povidone-iodine), and a 2-cm longitudinal midline incision was made. Submandibular salivary glands were dissected and retracted laterally to expose the carotid artery and right cervical vagus nerve. The vagus nerve was carefully dissected from the carotid artery and connected to platinum-iridium microelectrodes. Biopac MP150 system was used to deliver continuous electrical stimulation (5 V, 50 Hz, 100 ms) for 15 min. Heart rate was monitored during the procedure to ensure effective vagal stimulation. After the stimulation, tissues were returned to anatomical positions, and the neck was closed with a 6/0 suture. Mice were monitored for 30 min in an incubation chamber to ensure full recovery before returning them to the cage. Sham mice were intubated, a longitudinal neck incision was performed, and the glands were retracted without touching the vagus nerve to avoid mechanical stimulation. Vagal nerve stimulation was performed immediately before DSS treatment.

Splenectomy

Mice were anesthetized with isoflurane 5% and subjected to an abdominal incision on the epigastrium and mesogastrium. The spleen was exposed by gentle retraction of the stomach to the side as we described (*81*). The three main branches of the splenic artery were stabilized with nylon thread, ligated, and cut. The spleen was removed, and the abdominal wall was sutured with catgut and the skin with nylon thread. Mice were splenectomized 5 days before the experimental procedure.

Peritoneal lavage and bacterial load analysis

Peritoneal lavage was performed as we described (*82*). Six hours before euthanasia, mice were anesthetized with 5% isoflurane, the abdominal wall was disinfected with 70% ethanol, and 5 ml of sterile pyrogen-free PBS was injected intraperitoneally using a 25-gauge needle. Then, the abdomen was massaged for 1 min, and 1 ml of peritoneal fluid was aspirated using a sterile syringe. Peritoneal aspirates were centrifuged at 2000*g* for 20 min at 4°C, and supernatants were frozen at −20°C for further cytokine analysis. Peritoneal lavage bacterial load was analyzed as previously described (*83*). Freshly collected peritoneal aspirates were cultured in blood agar using a sterile inoculation loop, and agar plates were incubated at 37°C for 24 hours. Bacterial colonies (colony-forming units/ml of peritoneal aspirate) were counted using an ImageJ Fiji software cell analyzer (*84*).

Statistical analyses

Statistical analyses were performed with GraphPad Prism Software (GraphPad Software). The sample size was calculated on the basis of our preliminary results using G*Power3.1 and ANOVA (fixed effects, omnibus, one-way), assuming effect size = 0.25, $\alpha = 0.05$, power (1-β prob type II error) = 0.8. Data are expressed as mean ± SEM, and the figures represent experiments repeated twice on different days. The Student's *t* test or Mann-Whitney *U* test was used to compare two experimental groups. Three or more groups were analyzed with parametric one-way analysis of variance (ANOVA) with multiple pairwise comparisons. Normality and homogeneity of variance were confirmed with Kolmogorov-Smirnov analyses. Pair comparisons in nonparametric ANOVA tests were adjusted post hoc with the Tukey test (in equal sample sizes) or Bonferroni's for multiple hypothesis testing. The time courses and pairwise comparisons were analyzed with the two-way ANOVA for repeated measures. Statistical significance was established at $P \leq 0.05$ with a two-sided α. Figures show representative data of experiments that were replicated on different dates.

Supplementary Materials

The PDF file includes:
Materials and Methods
Figs. S1 to S7
Table S1
Legend for data file S1
References (*85*–*91*)

Other Supplementary Material for this manuscript includes the following:
Data file S1
MDAR Reproducibility Checklist

REFERENCES AND NOTES

1. G. P. Caviglia, A. Garrone, C. Bertolino, R. Vanni, E. Bretto, A. Poshnjari, E. Tribocco, S. Frara, A. Armandi, M. Astegiano, G. M. Saracco, L. Bertolusso, D. G. Ribaldone, Epidemiology of inflammatory bowel diseases: A population study in a healthcare district of north-west Italy. *J. Clin. Med.* **12**, 641 (2023).
2. N. A. Molodecky, I. S. Soon, D. M. Rabi, W. A. Ghali, M. Ferris, G. Chernoff, E. I. Benchimol, R. Panaccione, S. Ghosh, H. W. Barkema, G. G. Kaplan, Increasing incidence and prevalence of the inflammatory bowel diseases with time, based on systematic review. *Gastroenterology* **142**, 46–54.e42 (2012).
3. M. E. Kuenzig, D. G. Manuel, J. Donelle, E. I. Benchimol, Life expectancy and health-adjusted life expectancy in people with inflammatory bowel disease. *CMAJ* **192**, E1394–E1402 (2020).
4. M. Aldiabat, M. Yusuf, M. Al-Khateeb, Y. A. Jabiri, Sepsis in the settings of inflammatory bowel disease: Studying the outcomes of more than 8 million patients. *Chest* **162**, A661 (2022).
5. C. P. Selinger, J. M. Andrews, A. Titman, I. Norton, D. B. Jones, C. McDonald, G. Barr, W. Selby, R. W. Leong, Long-term follow-up reveals low incidence of colorectal cancer, but frequent need for resection, among Australian patients with inflammatory bowel disease. *Clin. Gastroenterol. Hepatol.* **12**, 644–650 (2014).
6. J. Marsal, M. Barreiro-de Acosta, I. Blumenstein, M. Cappello, T. Bazin, S. Sebastian, Management of non-response and loss of response to anti-tumor necrosis factor therapy in inflammatory bowel disease. *Front. Med.* **9**, 897936 (2022).
7. M. K.-L. Ko, S. C. Ng, L.-Y. Mak, M. K. Li, F. H. Lo, C. K. M. Ng, W. C. Lao, S. Tsang, K. H. Chan, Y. T. Hui, E. H. S. Shan, C. K. Loo, A. J. Hui, W. P. To, I. F. Hung, W. K. Leung, Infection-related hospitalizations in the first year after inflammatory bowel disease diagnosis. *J. Dig. Dis.* **17**, 610–617 (2016).
8. G. R. Lichtenstein, B. G. Feagan, R. D. Cohen, B. A. Salzberg, R. H. Diamond, D. M. Chen, M. L. Pritchard, W. J. Sandborn, Serious infections and mortality in association with therapies for Crohn's disease: TREAT registry. *Clin. Gastroenterol. Hepatol.* **4**, 621–630 (2006).
9. D. B. O'Connor, J. F. Thayer, K. Vedhara, Stress and health: A review of psychobiological processes. *Annu. Rev. Psychol.* **72**, 663–688 (2021).
10. H. Matsunaga, R. Hokari, T. Ueda, C. Kurihara, H. Hozumi, M. Higashiyama, Y. Okada, C. Watanabe, S. Komoto, M. Nakamura, A. Kawaguchi, S. Nagao, A. Sekiyama, S. Miura, Physiological stress exacerbates murine colitis by enhancing proinflammatory cytokine expression that is dependent on IL-18. *Am. J. Physiol. Gastrointest. Liver Physiol.* **301**, G555–G564 (2011).
11. V. A. Edgar, D. M. Silberman, G. A. Cremaschi, L. M. Zieher, A. M. Genaro, Altered lymphocyte catecholamine reactivity in mice subjected to chronic mild stress. *Biochem. Pharmacol.* **65**, 15–23 (2003).
12. K. A. James, J. I. Stromin, N. Steenkamp, M. I. Combrinck, Understanding the relationships between physiological and psychosocial stress, cortisol and cognition. *Front. Endocrinol.* **14**, 1085950 (2023).
13. S. W. Porges, Vagal tone: A physiologic marker of stress vulnerability. *Pediatrics* **90**, 498–504 (1992).
14. H. G. Kim, E. J. Cheon, D. S. Bai, Y. H. Lee, B. H. Koo, Stress and heart rate variability: A meta-analysis and review of the literature. *Psychiatry Investig.* **15**, 235–245 (2018).
15. R. Torres-Rosas, G. Yehia, G. Pena, P. Mishra, M. del Rocio Thompson-Bonilla, M. A. Moreno-Eutimio, L. A. Arriaga-Pizano, A. Isibasi, L. Ulloa, Dopamine mediates vagal modulation of the immune system by electroacupuncture. *Nat. Med.* **20**, 291–295 (2014).
16. J. M. Huston, M. Ochani, M. Rosas-Ballina, H. Liao, K. Ochani, V. A. Pavlov, M. Gallowitsch-Puerta, M. Ashok, C. J. Czura, B. Foxwell, K. J. Tracey, L. Ulloa, Splenectomy inactivates the cholinergic antiinflammatory pathway during lethal endotoxemia and polymicrobial sepsis. *J. Exp. Med.* **203**, 1623–1628 (2006).
17. H. Wang, M. Yu, M. Ochani, C. A. Amella, M. Tanovic, S. Susarla, J. H. Li, H. C. Wang, H. Yang, L. Ulloa, Y. Al-Abed, C. J. Czura, K. J. Tracey, Nicotinic acetylcholine receptor α7 subunit is an essential regulator of inflammation. *Nature* **421**, 384–388 (2003).
18. F. A. Koopman, S. S. Chavan, S. Miljko, S. Grazio, S. Sokolovic, P. R. Schuurman, A. D. Mehta, Y. A. Levine, M. Faltys, R. Zitnik, K. J. Tracey, P. P. Tak, Vagus nerve stimulation inhibits cytokine production and attenuates disease severity in rheumatoid arthritis. *Proc. Natl. Acad. Sci. U.S.A.* **113**, 8284–8289 (2016).
19. G. S. Bassi, A. Kanashiro, N. C. Coimbra, N. Terrando, W. Maixner, L. Ulloa, Anatomical and clinical implications of vagal modulation of the spleen. *Neurosci. Biobehav. Rev.* **112**, 363–373 (2020).
20. B. Bonaz, V. Sinniger, D. Hoffmann, D. Clarençon, N. Mathieu, C. Dantzer, L. Vercueil, C. Picq, C. Trocmé, P. Faure, J. L. Cracowski, S. Pellissier, Chronic vagus nerve stimulation in Crohn's disease: A 6-month follow-up pilot study. *Neurogastroenterol. Motil.* **28**, 948–953 (2016).
21. G. R. D'Haens, Z. Cabrijan, M. Eberhardson, R. M. van den Berg, M. Löwenberg, G. Fiorino, S. Danese, Y. A. Levine, D. Chernoff, Mo1906 – The effects of vagus nerve stimulation in biologicrefractory Crohn's disease: A prospective clinical trial. *Gastroenterology* **154**, S-847 (2018).
22. V. Sinniger, S. Pellissier, F. Fauvelle, C. Trocmé, D. Hoffmann, L. Vercueil, J. L. Cracowski, O. David, B. Bonaz, A 12-month pilot study outcomes of vagus nerve stimulation in Crohn's disease. *Neurogastroenterol. Motil.* **32**, e13911 (2020).
23. A. Youssef, B. K. Mohammed, A. Prasad, A. del Aguila, G. Bassi, W. Yang, L. Ulloa, Splenic SUMO1 controls systemic inflammation in experimental sepsis. *Front. Immunol.* **14**, 1200939 (2023).
24. S. A. Mustfa, M. Singh, A. Suhail, G. Mohapatra, S. Verma, D. Chakravorty, S. Rana, R. Rampal, A. Dhar, S. Saha, V. Ahuja, C. V. Srikanth, SUMOylation pathway alteration coupled with downregulation of SUMO E2 enzyme at mucosal epithelium modulates inflammation in inflammatory bowel disease. *Open Biol.* **7**, 170024 (2017).
25. J. Karhausen, J. D. Bernstock, K. R. Johnson, H. Sheng, Q. Ma, Y. Shen, W. Yang, J. M. Hallenbeck, W. Paschen, Ubc9 overexpression and SUMO1 deficiency blunt inflammation after intestinal ischemia/reperfusion. *Lab. Invest.* **98**, 799–813 (2018).
26. A. Decque, O. Joffre, J. G. Magalhaes, J.-C. Cossec, R. Blecher-Gonen, P. Lapaquette, A. Silvin, N. Manel, P.-E. Joubert, J.-S. Seeler, M. L. Albert, I. Amit, S. Amigorena, A. Dejean, Sumoylation coordinates the repression of inflammatory and anti-viral gene-expression programs during innate sensing. *Nat. Immunol.* **17**, 140–149 (2016).
27. K. Nacerddine, F. Lehembre, M. Bhaumik, J. Artus, M. Cohen-Tannoudji, C. Babinet, P. P. Pandolfi, A. Dejean, The SUMO pathway is essential for nuclear integrity and chromosome segregation in mice. *Dev. Cell* **9**, 769–779 (2005).
28. A. B. Celen, U. Sahin, Sumoylation on its 25th anniversary: Mechanisms, pathology, and emerging concepts. *FEBS J.* **287**, 3110–3140 (2020).
29. J.-S. Seeler, A. Dejean, SUMO and the robustness of cancer. *Nat. Rev. Cancer* **17**, 184–197 (2017).
30. B. Khan, L. V. Gand, M. Amrute-Nayak, A. Nayak, Emerging mechanisms of skeletal muscle homeostasis and cachexia: The SUMO perspective. *Cells* **12**, 644 (2023).
31. A. C. O. Vertegaal, Signalling mechanisms and cellular functions of SUMO. *Nat. Rev. Mol. Cell Biol.* **23**, 715–731 (2022).
32. K. Shiga, K. Izumi, K. Minato, T. Sugio, M. Yoshimura, M. Kitazawa, S. Hanashiro, K. Cortright, S. Kurokawa, Y. Momota, M. Sado, T. Maeno, T. Takebayashi, M. Mimura, T. Kishimoto, Subjective well-being and month-long LF/HF ratio among deskworkers. *PLOS ONE* **16**, e0257062 (2021).
33. B. Chassaing, J. D. Aitken, M. Malleshappa, M. Vijay-Kumar, Dextran sulfate sodium (DSS)-induced colitis in mice. *Curr. Protoc. Immunol.* **104**, 15.25.1–15.25.14 (2014).
34. L. Ulloa, Bioelectronic neuro-immunology: Neuronal networks for sympathetic-splenic and vagal-adrenal control. *Neuron* **111**, 10–14 (2023).
35. L. Ulloa, Electroacupuncture activates neurons to switch off inflammation. *Nature* **598**, 573–574 (2021).
36. H. Wang, H. Liao, M. Ochani, M. Justiniani, X. Lin, L. Yang, Y. Al-Abed, H. Wang, C. Metz, E. J. Miller, K. J. Tracey, L. Ulloa, Cholinergic agonists inhibit HMGB1 release and improve survival in experimental sepsis. *Nat. Med.* **10**, 1216–1221 (2004).
37. L. Ulloa, The vagus nerve and the nicotinic anti-inflammatory pathway. *Nat. Rev. Drug Discov.* **4**, 673–684 (2005).
38. L. Ulloa, The cholinergic anti-inflammatory pathway meets microRNA. *Cell Res.* **23**, 1249–1250 (2013).
39. W. Y. Cui, M. D. Li, Nicotinic modulation of innate immune pathways via α7 nicotinic acetylcholine receptor. *J. Neuroimmune Pharmacol.* **5**, 479–488 (2010).
40. R. D. Pullan, J. Rhodes, S. Ganesh, V. Mani, J. S. Morris, G. T. Williams, R. G. Newcombe, M. Russell, C. Feyerabend, G. Thomas, U. Sawe, Transdermal nicotine for active ulcerative colitis. *N. Engl. J. Med.* **330**, 811–815 (1994).
41. W. Yang, H. Sheng, J. W. Thompson, S. Zhao, L. Wang, P. Miao, X. Liu, M. A. Moseley, W. Paschen, Small ubiquitin-like modifier 3-modified proteome regulated by brain ischemia in novel small ubiquitin-like modifier transgenic mice: Putative protective proteins/pathways. *Stroke* **45**, 1115–1122 (2014).
42. J. Karhausen, L. Ulloa, W. Yang, SUMOylation connects cell stress responses and inflammatory control: Lessons from the gut as a model organ. *Front. Immunol.* **12**, 646633 (2021).

43. A. Dudek, D. Juric, A. Dowlati, U. Vaishampayan, H. Asaad, J. Rodon, B. Chao, B. Wang, J. Gibbs, V. Shinde, S. Friedlander, A. Berger, C. Ward, A. Martinez, R. Gharavi, A. Gomez-Pinillos, I. Proscurshim, A. Olszanski, First-in-human phase 1/2 study of the first-in-class SUMO-activating enzyme inhibitor TAK-981 in patients with advanced or metastatic solid tumors or relapsed/refractory lymphoma: Phase 1 results. *J. Immunother. Cancer* **9**, A505–A506 (2021).
44. A. Biederstädt, Z. Hassan, C. Schneeweis, M. Schick, L. Schneider, A. Muckenhuber, Y. Hong, G. Siegers, L. Nilsson, M. Wirth, Z. Dantes, K. Steiger, K. Schunck, P. Lenhof, A. Coluccio, F. Orben, J. Slawska, S. Langston, A. Scherger, D. Saur, S. Müller, R. Rad, W. Weichert, J. Nilsson, M. Reichert, G. Schneider, U. Keller, SUMO pathway inhibition targets an aggressive pancreatic cancer subtype. *Gut* **69**, 1472–1482 (2020).
45. S. Kumar, M. J. A. Schoonderwoerd, J. S. Kroonen, I. J. de Graaf, M. Sluijter, D. Ruano, R. González-Prieto, M. Verlaan-de Vries, J. Rip, R. Arens, N. F. C. C. de Miranda, L. J. A. C. Hawinkels, T. van Hall, A. C. O. Vertegaal, Targeting pancreatic cancer by TAK-981: A SUMOylation inhibitor that activates the immune system and blocks cancer cell cycle progression in a preclinical model. *Gut* **71**, 2266–2283 (2022).
46. A. Sazonovs, C. R. Stevens, G. R. Venkataraman, K. Yuan, B. Avila, M. T. Abreu, T. Ahmad, M. Allez, A. N. Ananthakrishnan, G. Atzmon, A. Baras, J. C. Barrett, N. Barzilai, L. Beaugerie, A. Beecham, C. N. Bernstein, A. Bitton, B. Bokemeyer, A. Chan, D. Chung, I. Cleynen, J. Cosnes, D. J. Cutler, A. Daly, O. M. Damas, L. W. Datta, N. Dawany, M. Devoto, S. Dodge, E. Ellinghaus, L. Fachal, M. Farkkila, W. Faubion, M. Ferreira, D. Franchimont, S. B. Gabriel, T. Ge, M. Georges, K. Gettler, M. Giri, B. Glaser, S. Goerg, P. Goyette, D. Graham, E. Hämäläinen, T. Haritunians, G. A. Heap, M. Hiltunen, M. Hoeppner, J. E. Horowitz, P. Irving, V. Iyer, C. Jalas, J. Kelsen, H. Khalili, B. S. Kirschner, K. Kontula, J. T. Koskela, S. Kugathasan, J. Kupcinskas, C. A. Lamb, M. Laudes, C. Lévesque, A. P. Levine, J. D. Lewis, C. Liefferinckx, B. S. Loescher, E. Louis, J. Mansfield, S. May, J. L. McCauley, E. Mengesha, M. Mni, P. Moayyedi, C. J. Moran, R. D. Newberry, S. O'Charoen, D. T. Okou, B. Oldenburg, H. Ostrer, A. Palotie, J. Paquette, J. Pekow, I. Peter, M. J. Pierik, C. Y. Ponsioen, N. Pontikos, N. Prescott, A. E. Pulver, S. Rahmouni, D. L. Rice, P. Saavalainen, B. Sands, R. B. Sartor, E. R. Schiff, S. Schreiber, L. P. Schumm, A. W. Segal, P. Seksik, R. Shawky, S. Z. Sheikh, M. S. Silverberg, A. Simmons, J. Skeiceviciene, H. Sokol, M. Solomonson, H. Somineni, D. Sun, S. Targan, D. Turner, H. H. Uhlig, A. E. van der Meulen, S. Vermeire, S. Verstockt, M. D. Voskuil, H. S. Winter, J. Young, Belgium IBD Consortium, Cedars-Sinai IBD, International IBD Genetics Consortium, NIDDK IBD Genetics Consortium, NIHR IBD BioResource, Regeneron Genetics Center, SHARE Consortium, SPARC IBD Network, UK IBD Genetics Consortium, R. H. Duerr, A. Franke, S. R. Brant, J. Cho, R. K. Weersma, M. Parkes, R. J. Xavier, M. A. Rivas, J. D. Rioux, D. P. B. McGovern, H. Huang, C. A. Anderson, M. J. Daly, Large-scale sequencing identifies multiple genes and rare variants associated with Crohn's disease susceptibility. *Nat. Genet.* **54**, 1275–1283 (2022).
47. F. P. Zhang, L. Mikkonen, J. Toppari, J. J. Palvimo, I. Thesleff, O. A. Jänne, Sumo-1 function is dispensable in normal mouse development. *Mol. Cell. Biol.* **28**, 5381–5390 (2008).
48. L. Wang, C. Wansleeben, S. Zhao, P. Miao, W. Paschen, W. Yang, SUMO2 is essential while SUMO3 is dispensable for mouse embryonic development. *EMBO Rep.* **15**, 878–885 (2014).
49. E. Meroni, N. Stakenborg, P. J. Gomez-Pinilla, M. Stakenborg, J. Aguilera-Lizarraga, M. Florens, M. Delfini, V. de Simone, G. De Hertogh, G. Goverse, G. Matteoli, G. E. Boeckxstaens, Vagus nerve stimulation promotes epithelial proliferation and controls colon monocyte infiltration during DSS-induced colitis. *Front. Med.* **8**, 694268 (2021).
50. K. Asano, N. Takahashi, M. Ushiki, M. Monya, F. Aihara, E. Kuboki, S. Moriyama, M. Iida, H. Kitamura, C. H. Qiu, T. Watanabe, M. Tanaka, Intestinal CD169^{+} macrophages initiate mucosal inflammation by secreting CCL8 that recruits inflammatory monocytes. *Nat. Commun.* **6**, 7802 (2015).
51. E. S. Lightcap, P. Yu, S. Grossman, K. Song, M. Khattar, K. Xega, X. He, J. M. Gavin, H. Imaichi, J. J. Garnsey, E. Koenig, H. Zhang, Z. Lu, P. Shah, Y. Fu, M. A. Milhollen, B. A. Hatton, J. Riceberg, V. Shinde, C. Li, J. Minissale, X. Yang, D. England, R. A. Klinghoffer, S. Langston, K. Galvin, G. Shapiro, S. M. Pulukuri, S. Y. Fuchs, D. Huszar, A small-molecule SUMOylation inhibitor activates antitumor immune responses and potentiates immune therapies in preclinical models. *Sci. Transl. Med.* **13**, eaba7791 (2021).
52. K. Gerlach, Y. Hwang, A. Nikolaev, R. Atreya, H. Dornhoff, S. Steiner, H.-A. Lehr, S. Wirtz, M. Vieth, A. Waisman, F. Rosenbauer, A. N. J. McKenzie, B. Weigmann, M. F. Neurath, TH9 cells that express the transcription factor PU.1 drive T cell–mediated colitis via IL-9 receptor signaling in intestinal epithelial cells. *Nat. Immunol.* **15**, 676–686 (2014).
53. E. Meroni, N. Stakenborg, P. J. Gomez-Pinilla, G. De Hertogh, G. Goverse, G. Matteoli, S. Verheijden, G. E. Boeckxstaens, Functional characterization of oxazolone-induced colitis and survival improvement by vagus nerve stimulation. *PLOS ONE* **13**, e0197487 (2018).
54. B. S. McEwen, Protective and damaging effects of stress mediators. *N. Engl. J. Med.* **338**, 171–179 (1998).
55. L. Frick, M. Barreiro Arcos, M. Rapanelli, M. Zappia, M. Brocco, C. Mongini, A. Genaro, G. Cremaschi, Chronic restraint stress impairs T-cell immunity and promotes tumor progression in mice. *Stress* **12**, 134–143 (2009).
56. Z. Feng, L. Liu, C. Zhang, T. Zheng, J. Wang, M. Lin, Y. Zhao, X. Wang, A. J. Levine, W. Hu, Chronic restraint stress attenuates p53 function and promotes tumorigenesis. *Proc. Natl. Acad. Sci. U.S.A.* **109**, 7013–7018 (2012).
57. C. Abe, T. Inoue, M. A. Inglis, K. E. Viar, L. Huang, H. Ye, D. L. Rosin, R. L. Stornetta, M. D. Okusa, P. G. Guyenet, C1 neurons mediate a stress-induced anti-inflammatory reflex in mice. *Nat. Neurosci.* **20**, 700–707 (2017).
58. P. Sun, K. Zhou, S. Wang, P. Li, S. Chen, G. Lin, Y. Zhao, T. Wang, Involvement of MAPK/NF-κB signaling in the activation of the cholinergic anti-inflammatory pathway in experimental colitis by chronic vagus nerve stimulation. *PLOS ONE* **8**, e69424 (2013).
59. J. Meregnani, D. Clarencon, M. Vivier, A. Peinnequin, C. Mouret, V. Sinniger, C. Picq, A. Job, F. Canini, M. Jacquier-Sarlin, B. Bonaz, Anti-inflammatory effect of vagus nerve stimulation in a rat model of inflammatory bowel disease. *Auton. Neurosci.* **160**, 82–89 (2011).
60. R. Kühn, J. Löhler, D. Rennick, K. Rajewsky, W. Müller, Interleukin-10-deficient mice develop chronic enterocolitis. *Cell* **75**, 263–274 (1993).
61. L. Ulloa, S. Quiroz-Gonzalez, R. Torres-Rosas, Nerve stimulation: Immunomodulation and control of inflammation. *Trends Mol. Med.* **23**, 1103–1120 (2017).
62. S. Li, J. Huang, Y. Guo, J. Wang, S. Lu, B. Wang, Y. Gong, S. Qin, S. Zhao, S. Wang, Y. Liu, Y. Fang, Y. Guo, Z. Xu, L. Ulloa, PAC1 receptor mediates electroacupuncture-induced neuro and immune protection during cisplatin chemotherapy. *Front. Immunol.* **12**, 714244 (2021).
63. R. L. Bandoni, P. N. Bricher Choque, H. Dellê, T. L. de Moraes, M. H. M. Porter, B. D. da Silva, G. A. Neves, M. C. Irigoyen, K. De Angelis, V. A. Pavlov, L. Ulloa, F. M. Consolim-Colombo, Cholinergic stimulation with pyridostigmine modulates a heart-spleen axis after acute myocardial infarction in spontaneous hypertensive rats. *Sci. Rep.* **11**, 9563 (2021).
64. H. Tang, S. Qin, W. Li, X. Chen, L. Ulloa, Q. Zhu, B. Liu, Y. Gong, Y. Zhao, S. Wang, S. Li, Y. Guo, Z. Xu, Y. Guo, P2RX7 in dopaminergic neurons of ventral periaqueductal gray mediates HTWP acupuncture-induced consciousness in traumatic brain injury. *Front. Cell. Neurosci.* **14**, 598198 (2020).
65. K. Kawashima, M. Onizawa, T. Fujiwara, N. Gunji, H. Imamura, K. Katakura, H. Ohira, Evaluation of the relationship between the spleen volume and the disease activity in ulcerative colitis and Crohn disease. *Medicine* **101**, e28515 (2022).
66. S. Calzado, M. Navarro, I. Puig, B. Font, Splenic abscess as the first manifestation of Crohn's disease. *J. Crohns Colitis* **4**, 703–704 (2010).
67. A. F. Muller, E. Cornford, P. J. Toghill, Splenic function in inflammatory bowel disease: Assessment by differential interference microscopy and splenic ultrasound. *Q. J. Med.* **86**, 333–340 (1993).
68. J. M. Desterro, M. S. Rodriguez, R. T. Hay, SUMO-1 modification of IκBα inhibits NF-κB activation. *Mol. Cell* **2**, 233–239 (1998).
69. X. Han, X. X. Dong, M. Y. Shi, L. Feng, X. L. Wang, J. S. Zhang, Q. C. Yan, SUMOylation and deacetylation affect NF-κB p65 activity induced by high glucose in human lens epithelial cells. *Int. J. Ophthalmol.* **12**, 1371–1379 (2019).
70. C.-H. Huang, T.-T. Yang, K.-I. Lin, Mechanisms and functions of SUMOylation in health and disease: A review focusing on immune cells. *J. Biomed. Sci.* **31**, 16 (2024).
71. A. Tahiri, A. Youssef, R. Inoue, S. Moon, L. Alsarkhi, L. Berroug, X. T. A. Nguyen, L. Wang, H. Kwon, Z. P. Pang, J. Y. Zhao, J. Shirakawa, L. Ulloa, A. E. Ouaamari, Vagal sensory neuron-derived FGF3 controls insulin secretion. *Dev. Cell* 10.1016/j.devcel.2024.09.016 (2024).
72. C. Bauer, P. Duewell, C. Mayer, H. A. Lehr, K. A. Fitzgerald, M. Dauer, J. Tschopp, S. Endres, E. Latz, M. Schnurr, Colitis induced in mice with dextran sulfate sodium (DSS) is mediated by the NLRP3 inflammasome. *Gut* **59**, 1192–1199 (2010).
73. J. J. Kim, M. S. Shajib, M. M. Manocha, W. I. Khan, Investigating intestinal inflammation in DSS-induced model of IBD. *J. Vis. Exp.* **60**, 3678 (2012).
74. A. Nakajima, T. Shibuya, T. Sasaki, Y. J. Lu, D. Ishikawa, K. Haga, M. Takahashi, N. Kaga, T. Osada, N. Sato, A. Nagahara, Nicotine oral administration attenuates DSS-induced colitis through upregulation of indole in the distal colon and rectum in mice. *Front. Med.* **8**, 789037 (2021).
75. E. Antoniou, G. A. Margonis, A. Angelou, A. Pikouli, P. Argiri, I. Karavokyros, A. Papalois, E. Pikoulis, The TNBS-induced colitis animal model: An overview. *Ann. Med. Surg.* **11**, 9–15 (2016).
76. F. Scheiffele, I. J. Fuss, Induction of TNBS colitis in mice. *Curr. Protoc. Immunol.* **49**, 15.19.11–15.19.14 (2002).
77. F. Heller, I. J. Fuss, E. E. Nieuwenhuis, R. S. Blumberg, W. Strober, Oxazolone colitis, a Th2 colitis model resembling ulcerative colitis, is mediated by IL-13-producing NK-T cells. *Immunity* **17**, 629–638 (2002).
78. L. Peng, X. Gao, L. Nie, J. Xie, T. Dai, C. Shi, L. Tao, Y. Wang, Y. Tian, J. Sheng, Astragalin attenuates dextran sulfate sodium (DSS)-induced acute experimental colitis by alleviating gut microbiota dysbiosis and inhibiting NF-κB activation in mice. *Front. Immunol.* **11**, 2058 (2020).
79. B.-R. Li, J. Wu, H.-S. Li, Z.-H. Jiang, X.-M. Zhou, C.-H. Xu, N. Ding, J.-M. Zha, W.-Q. He, In vitro and in vivo approaches to determine intestinal epithelial cell permeability. *J. Vis. Exp.* **19**, 57032 (2018).

80. P. N. Bricher Choque, R. P. Vieira, L. Ulloa, C. Grabulosa, M. C. Irigoyen, K. De Angelis, A. P. Ligeiro De Oliveira, K. J. Tracey, V. A. Pavlov, F. M. Consolim-Colombo, The cholinergic drug pyridostigmine alleviates inflammation during LPS-induced acute respiratory distress syndrome. *Front. Pharmacol.* **12**, 624895 (2021).
81. B. Joseph, G. Shimojo, Z. Li, M. R. Thompson-bonilla, R. Shah, A. Kanashiro, H. C. Salgado, L. Ulloa, Glucose activates vagal control of hyperglycemia and inflammation in fasted mice. *Sci. Rep.* **9**, 1012 (2019).
82. A. Ray, B. N. Dittel, Isolation of mouse peritoneal cavity cells. *J. Vis. Exp.* 1488 (2010).
83. S. Maier, T. Traeger, M. Entleutner, A. Westerholt, B. Kleist, N. Hüser, B. Holzmann, A. Stier, K. Pfeffer, C.-D. Heidecke, Cecal ligation and puncture versus colon ascendens stent peritonitis: Two distinct animal models for polymicrobial sepsis. *Shock* **21**, 505–511 (2004).
84. J. Schindelin, I. Arganda-Carreras, E. Frise, V. Kaynig, M. Longair, T. Pietzsch, S. Preibisch, C. Rueden, S. Saalfeld, B. Schmid, Fiji: An open-source platform for biological-image analysis. *Nat. Methods* **9**, 676–682 (2012).
85. M. Kanke, M. M. Kennedy Ng, S. Connelly, M. Singh, M. Schaner, M. T. Shanahan, E. A. Wolber, C. Beasley, G. Lian, A. Jain, M. D. Long, E. L. Barnes, H. H. Herfarth, K. L. Isaacs, J. J. Hansen, M. Kapadia, J. G. Guillem, C. Feschotte, T. S. Furey, S. Z. Sheikh, P. Sethupathy, Single-cell analysis reveals unexpected cellular changes and transposon expression signatures in the colonic epithelium of treatment-naïve adult Crohn's disease patients. *Cell. Mol. Gastroenterol. Hepatol.* **13**, 1717–1740 (2022).
86. J. B. de Souza, U. Okomo, N. D. Alexander, N. Aziz, B. M. J. Owens, H. Kaur, M. Jasseh, S. Muangnoicharoen, P. F. Sumariwalla, D. C. Warhurst, S. A. Ward, D. J. Conway, L. Ulloa, K. J. Tracey, B. M. J. Foxwell, P. M. Kaye, M. Walther, Oral activated charcoal prevents experimental cerebral malaria in mice and in a randomized controlled clinical trial in man did not interfere with the pharmacokinetics of parenteral artesunate. *PLOS ONE* **5**, e9867 (2010).
87. A. U. Rehman, N. Z. Siddiqui, N. A. Farooqui, G. Alam, A. Gul, B. Ahmad, M. Asim, A. I. Khan, Y. Xin, W. Zexu, H. Song Ju, W. Xin, S. Lei, L. Wang, *Morchella esculenta* mushroom polysaccharide attenuates diabetes and modulates intestinal permeability and gut microbiota in a type 2 diabetic mice model. *Front. Nutr.* **9**, 984695 (2022).
88. S. Wirtz, C. Neufert, B. Weigmann, M. F. Neurath, Chemically induced mouse models of intestinal inflammation. *Nat. Protoc.* **2**, 541–546 (2007).
89. E. Park, M. A. Evans, H. Doviak, K. Horitani, H. Ogawa, Y. Yura, Y. Wang, S. Sano, K. Walsh, Bone marrow transplantation procedures in mice to study clonal hematopoiesis. *J. Vis. Exp.* **171**, e61875 (2021).
90. T. S. Furey, P. Sethupathy, S. Z. Sheikh, Redefining the IBDs using genome-scale molecular phenotyping. *Nat. Rev. Gastroenterol. Hepatol.* **16**, 296–311 (2019).
91. B. P. Keith, J. B. Barrow, T. Toyonaga, N. Kazgan, M. H. O'Connor, N. D. Shah, M. S. Schaner, E. A. Wolber, O. K. Trad, G. R. Gipson, W. A. Pitman, M. Kanke, S. J. Saxena, N. Chaumont, T. S. Sadiq, M. J. Koruda, P. A. Cotney, N. Allbritton, D. G. Trembath, F. Sylvester, T. S. Furey, P. Sethupathy, S. Z. Sheikh, Colonic epithelial miR-31 associates with the development of Crohn's phenotypes. *JCI Insight* **3**, e122788 (2018).

Acknowledgments: We thank P. Miao and the Core Microscopy Facility of Duke University for technical assistance. **Funding:** A.Y., A.U.R., W.Y., J.K., and L.U. are funded by NIH NCCIH-AT011387. S.Z.S. is funded by NIDDK (P01DK094779, 1R01DK104828, and P30-DK034987) and the Helmsley Charitable Trust. **Author contributions:** A.Y., A.U.R., and M.E. performed experiments, analyzed data, and prepared figures. J.R. contributed to IL-10 analyses. S.Z.S. and J.K. performed human clinical sample analyses. W.Y. participated in experimental design and data interpretation. L.U. designed and directed the study and wrote the article. All authors participated in the design of the study, data interpretation, and presentation and approved the manuscript. **Competing interests:** L.U. and W.Y. are inventors on a patent application (#PCT/US2024/039542) entitled "SUMOylation as a therapeutic target in inflammatory bowel diseases and infectious disorders" submitted by Duke University. The other authors declare that they have no competing interests. **Data and materials availability:** All data associated with this study are present in the paper or the supplementary materials. Mouse strains and plasmids can be provided by W.Y. through a completed material transfer agreement. Requests for the materials should be submitted to W.Y. (wei.yang.@duke.edu).

Submitted 5 October 2023
Resubmitted 21 June 2024
Accepted 31 October 2024
Published 20 November 2024
10.1126/scitranslmed.adl2184